POLITECNICO DI TORINO

Corso di Laurea Magistrale in Ingegneria Civile

A Finite Fracture Mechanics approach to brittle crack initiation from circular holes

Relatori:

Prof. Alberto Giuseppe Sapora

Prof. Pietro Cornetti

Candidata:

Francesca Condemi

A.A. 2016/2017

Contents

Summary

In this work the coupled Finite Fracture Mechanics criterion is applied to investigate the brittle crack initiation in structures containing a circular hole under mode I loading conditions. The analysis involves the implementation of the stress field and stress intensity factor functions already proposed in literature. The accuracy of these expressions are verified numerically through a finite element analysis by ANSYS ® code. Theoretical FFM prediction are compared with experimental results on two different polymeric materials: PMMA and GPPS.
The agreement is found to be generally satisfactory, confirming the potentialities of FFM in the framework of Fracture Mechanics.

Sommario

Nella presente tesi è stato utilizzato il criterio della Meccanica della Frattura Finita (FFM) per studiare la propagazione di crack in strutture fragili contenenti un foro circolare e caricate in modo I. L'analisi comprende l'implementazione del campo tensionale e della funzioni che descrivono il fattore di intensificazione degli sforzi già presenti in letteratura. L'accuratezza di queste espressioni è stata verificata numericamente tramite un' analisi agli elementi finiti condotta attraverso l'uso del software ANSYS ®. Le previsioni teoriche, derivanti dall'applicazione della FFM, sono state confrontate con i risultati sperimentali realizzati su due differenti materiali polimerici: il PMMA e il GPPS.
L'accordo tra previsioni teoriche e dati sperimentali è risultato più che soddisfacente, confermando le potenzialità della FFM nell'ambito della Meccanica della Frattura fragile.

Dedication

To mum and dad that have made all of this possible with their sacrifices.
To Professor Alberto Sapora that has guided me in the world of the Fracture Mechanics.

"Successful engineering is all about how things break or break."
(Henry Petroski)

CHAPTER 1

Introduction

Fracture Mechanics investigates the failure behavior of structural elements. As a matter of fact, the strength of structures decreases in presence of defects such as cracks, notches, holes. Fracture can be present and can be studied over different scales from nanoscale (10 times the average dimension of atoms) to macroscale. No higher scales are generally considered. Most of the time, microcracks propagate due to fatigue, i.e. the application of cyclical loads; they grow, coalesce and, for subsequent phases, increasing fractures are formed and in this way it is possible to pass from the analysis of an integer solid to the one that presents microcracks and, then, macrocracks. The definition of resistence has to be reviewed in order to consider not only the tensile strength as it can only quantify the particle's resistance to an applied load (not considering inherent flaws present in brittle materials or the concentration of the stresses around these flaws when the material is loaded and their effect to the fracture process). Hence another parameter has to be introduced and it is the force that opposes itself to the propagation of the crack, i.e. the toughness to fracture. Fracture toughness is an intrinsic material property and is defined as a measure of the energy required to create a new surface in a material. It represents a sort of critical value of the Stress Intensity Factor (SIF). The SIF is used in fracture mechanics to predict the stress state near the tip of a crack caused by a remote load or residual stresses. The magnitude of SIF depends on sample geometry, the size and the location of the crack, the magnitude and the modal distribution of the loads on the material. Also the already quoted scale of the analysis, is a key feature. Therefore, basing

on their behavior, it is possible to distinguish two kind of materials: the first shows high strength but low toughness and it represents the class of brittle materials (once there is a crack, this propagates with high speed until the failure of the body); the second, instead, presents lower strength but high toughness and in this case we talk about ductile materials. So fracture studies have been profoundly changed in the last years by the focus on structural element sensitivity to defects and size scale effect. Obviously a foundamental step that has to be taken into account is a proper stress analysis including the stress concentration whatever the crack propagation mechanism is.
The evaluation of the stress field in a structural body due to the presence of a crack can be obtained within the linear elastic theory. Obviously a great attention has to be paid concerning the high stresses surrounding the crack-tip and to the probably presence of plasticization phenomena and other non linear effect. In spite of this linear elastic stress analysis can be defined as the fundamental base of the moste current fracture studies if the small scale yielding hypotesis is respected. In this case non linear effects are limitated to a small region in the surroundings of the crack-tip while the remaining portion is characterized by the linear elastic field.
The theory of linear elastic fracture mechanics (LEFM) was firstly developed by Griffith and Irwin and it was able to predict the behaviour of bodies containing cracks in terms of brittle fracture. For what concerns the studies underlying in this thesis, a brittle fracture can be defined as any sudden failure caused by the propagation of cracks due to the application of monotonically increasing loadings. However the LEFM is a field that presents some limitations. Indeed, the traditional stress approach provides good results for crack-free bodies and the energetic approach gives good results for large cracks bodies while for intermediate conditions (small cracks, notches, holes) both approaches fail.

In order to overcome these limitations and to propose a more generally applicable method a new approach have been successfully developed by introducing an internal material length Δ. The value of Δ is obtained by imposing the fulfilment of the two limit cases: long crack failure load for the stress criterion and no crack failure load for the energetic criterion. On the other hand the two mentioned failure criteria remain distinct and in general it can be asserted that the fulfilment of one implies the violation of the other one. Nevertheless it is possible to couple these two approaches. In this case Δ is no more a material parameter, but it becomes a structural one. A more detailed explanation of this concepts is the main character of Chapter 2 about Finite Fracture Mechanics, which shows the limits of the LEFM and the classical theories and puts in evidence the strengths of this new evoluted method.

Once defined the theoretical basis, the attention will be focused on practical studies. In Chapter 3 precise complutational analysis to evaluate the stress field and the stress intensity factor functions well determined infinite geometries will be presented. The bodies under consideration show defects (a central hole) characterized by different dimensions. Two different materials and two different loading conditions are taken into account. The obtained predictions are in good agreement with those available in the literature.

In Chapter 4 the experimental tests conducted by an external team of researchers on two different materials, PMMA and GPPS, will be described. Two different typologies of test were carried out: the first one is the traditional brazilian disk test on circular specimens, generally used in geothecnical studies, to investigate the strength of rock materials. The second one is the classical tensile test on rectangular samples, generally used for metallic material components studies. Both tests involved PMMA and GPPS considering, at least, four different hole sizes. They were small enough to apply the same analysis derived from infinite geometries. Thanks to the tests it was possible to evaluate the failure load and a comparison between numerical simulation outputs and experimental ones is provided. The great agreement between them is demonstrated by the low percentage of error obtained.

Finally, some final considerations will be presented. Indeed the final chapter goal is to put in evidence how useful can be the application of the finite element analysis if the modeler knowledge of the dynamics of representation is suitable and above all how the finite fracture mechanics has revolutionized not only the way of approaching to the brittle failure of bodies containing flaws and defects.

CHAPTER 2

Finite Fracture Mechanics

2.1 Introduction

Fracture Mechanics is the science which describes the failure behavior of bodies containing defects. Generally, it can be stated that fracture is determined by local stress concentrations and, knowing its development, the sudden failures in structural bodies can be avoided. It is shown that, under certain well-defined conditions, crack propagation can be predicted using linear elastic analysis. In this case the field under attention is the so called Linear Elastic Fracture Mechanics (LEFM). The conditions necessary for brittle failure can be foreseen but only assuming that a crack already exists. If the crack is already there it has to merely consider its propagation. Two are the failure criteria provided by LEFM: the first based on the stress field study, and the second concerning energetic assumptions. But the two approaches works well in the two opposite situations; in fact the first one provides good results for bodies without cracks and the second one considering elements characterized by enough large cracks. The lack of satisfaction, respectively, of the two restrainments implies the failure of them and the birth of singularities. According to the stress criterion, it can be asserted that the failure takes place if, at least in one point, the maximum principal stress reaches the tensile strength:

$$\sigma = \sigma_u \tag{2.1}$$

Yet the application of this principle provides a null failure load (singular stress field in front of the crack tip) for a body containing a crack. For what concern, instead, the energetic criterion, it states that the failure occurs when the crack driving force G equals the crack resistance G_f:

$$G = G_f \tag{2.2}$$

G is defined as the strain energy released for a unitary increment of the fracture area and it is called *strain energy release rate* while G_f, *the fracture energy*, is the energy needed to create the unit fracture surface and it is a property of the material. Indeed, applying the Irwin relation (1957):

$$G = \frac{K_I^2}{E} \qquad G_f = \frac{K_{IC}^2}{E} \tag{2.3}$$

the Eq.(2.2) can be rewritten equivanlenty and it can be said that the failure is achieved when:

$$K_I = K_{IC} \tag{2.4}$$

where K_I is the SIF and K_{IC} the Fracture Thoughness. But the imposition of Eq.(2.2) to crack free elements gives infinite failure load, being the stress intensity factor zero in absence of crack.
Therefore the criteria work for the extreme cases and problems arise if they are applied to intermediate cases (for example short cracks, notches and holes). As solution for this drawback the methodology of the Theory of the Critical Distance (TCD) can be exploited. The TCD is not one method but a group of methods which have certain features in common, principally the use of a characteristic material length parameter, the critical distance Δ, and the use of linear elastic analysis. The simpler Point Method (PM), or *point-wise stress criterion* and the slightly more complex method Line Method (LM), or *average stress criterion*, are analyzed. These methods calculate a stress value and equate it to a characteristic strenght for the material. The advantage is to obtain analytical results for sufficiently ordinary geometries or to couple the failure criterion with a linear elastic analysis performed numerically by the finite element method. The task of the characteristic lenght is to take into account the fracture thoughness for stress based criteria and the tensile strength for energy based criteria. The aim is to show how predictions of brittle fracture can be made very easily, for situations where the elastic stress field around the stress concentration feature is known, for example from FEA.

2.2 Stress and energy based approaches

It is possible to consider two different tipologies of specimens: a circular and a rectangular plate. The first is loaded by a compressive force P and has two symmetric cracks with an extension equal to a (with $a \geq 0$) in the direction of the application of the force. The second is loaded by a tensile force P and has two symmetric cracks of length a in the direction orthogonal to the one of the application of the load. For the sake of simplicity only the failure mode I is analyzed:

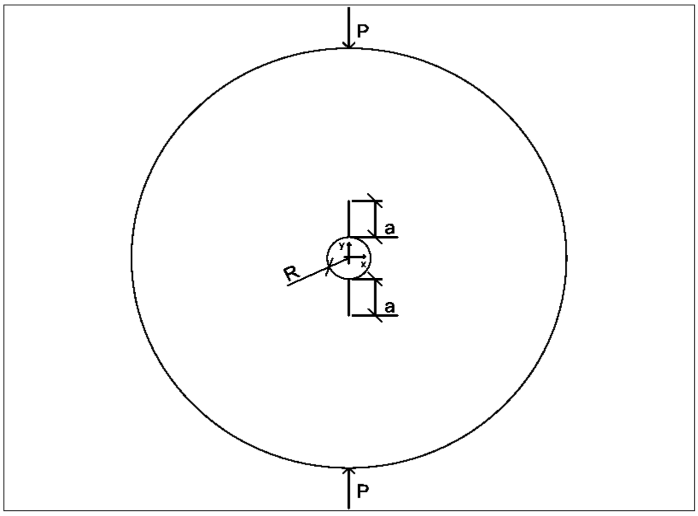

Figure 2.1: BD geometry

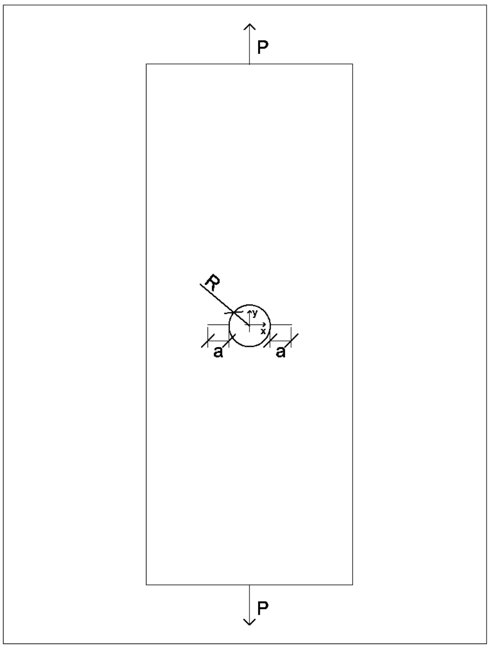

Figure 2.2: Tensile plate geometry

It has been said that it is possible to consider two different methods to achieve the same goal, the *point-wise stress criterion* and the *average stress criterion*. Considering the first one, failure occurs when the stress at a distance Δ_{PS} attains the tensile strength σ_u. Instead, referring to the latter criterion, failure happens when the average stress achieves the critical value σ_u ahead of the crack-tip over a Δ_{LS} long segment from the hole. They can be written respectively:

$$\sigma_x(R + \Delta_{PS}) = \sigma_u \tag{2.5}$$

$$\int_R^{R+\Delta_{LS}} \sigma_x(y)dy = \sigma_u \Delta_{LS} \tag{2.6}$$

Obviously PS and LS stand for "point-wise stress" and "line stress" respectively. Both these criteria if applied to crack free sample give the Eq.(2.1). Instead, if Eq.(2.5) are applied to bodies with a relatively large crack (i.e. $\Delta \ll a$) the characteristic lenghts can be determined. In this case only the asymptotic stress field at the crack-tip is required:

$$\sigma_x(y) = \frac{K_I}{\sqrt{2\pi y}} \tag{2.7}$$

Substituting Eq.(2.7) in Eq.(2.6) the critical distance can be obtained:

$$\Delta_{LS} = \frac{2}{\pi}\left(\frac{K_{IC}}{\sigma_u}\right)^2 \tag{2.8}$$

If a theoretical solution for the stress field is not available, a numerically achieved one can be introduced in Eq.(2.6) derived by a FEA. Generally, this is required when complex geometries in the intermediate cases (between no cracks and large cracks) are studied because the exact stress field is necessary. This is the way to achieve exact solution since the stress field is not available in literature.
For what concern the failure of specimens, in case of plain samples, it can be assumed that the collapse is reached when the energy available during an extension of the crack, Δ_{LE}, attains the critical value $G_f\Delta_{LE}$. So the modification of the LEFM leads to the same result of the stress criterion. In formulae:

$$\int_0^{\Delta_{LE}} G(a)da = G_f\Delta_{LE} \tag{2.9}$$

or considering the Irwin relationship:

$$\int_0^{\Delta_{LE}} K_I^2(a)da = K_{IC}^2\Delta_{LE} \tag{2.10}$$

If specimens with $\Delta_{LE} \ll a$ are considerd this method corresponds to the application of Eq.(2.4). On the other hand, imposing Eq.(2.1) for a $a = 0$ the critical distance is again obtained:

$$\Delta_{LE} = \frac{2}{\pi}\left(\frac{K_{IC}}{c\sigma_u}\right)^2 \tag{2.11}$$

having substitued the value of the stress intensity factor with the expression:

$$K_I(a) = c\sigma\sqrt{\pi a} \tag{2.12}$$

where c is a dimensionless parameter that depends on the location of the crack and it is equal to 1 for a centered crack. In this last case the Eq. (2.8) and (2.11) are the same. Even if the stress and the energy criterion are pretty similar, from a computational point of view, the last one is the most suitable because the SIF values are obtainable from handbooks or specific LEFM codes. On the contrary, the stress function $\sigma_x(y)$ usually is not inferable analitically and so it has to be calculated for each value of a. Therefore with the application of Eq.(2.10) only one function, $K_I(a)$ is necessary for every value of a to get the critical load.

The critical distance, regardless how it is evaluated (application of Eq.(2.8) or (2.11)), is a structural parameter which describes the material brittleness. Small values of Δ are indicative of a brittle behavior and viceversa, the large ones are clue of a ductile behavior ruled by Eq.(2.1).

The predictions of the PM and LM are identical for long cracks and, trivially, for plain tensile specimens. Still it is not guaranteed that the predictions are identical for any other problem. However the differences between the PM and LM results are almost always small. The first method can be accurated in some cases and the second in others. This may be related to the operative mechanism of failure. In any case the differences in the results, between PM and LM, are so small that both are proper to describe experimental data that inevitably contains a certain amount of scatter.

The most important peculiarity that has to be pointed out from the study of the average stress and energy criteria is their physical meaning: with finite fracture mechanics it can be asserted that fracture does not propagate continuosly but through finite crack extensions (FCE), at least at the first step, whose length is a material constant. It has been said that the predictions of the two criteria are very similar but not identical and in fact it is not possible to obtain the stress intensity factor from the stress field, for any crack extension, and viceversa. On the criteria (2.6) and (2.9) the FFM approach is founded. This approach can not give continuos crack growth but almost all the fracture processes are characterized by a discontinuos crack growth (talking about polymers for example). The crack discontinuities are probably connected to the microstructure features of the materials and, being not fully understood yet, the finite extension of a crack is assumed *a priori*. The FFM criterion can be applied to all classes of materials and at all size scales. The Eq.(2.6) and (2.10) generally provide results in good agreement with experimental data but they still contains some defects. The flaws can be noticed if specimens whose structural size is comparable to the finite crack extensions are analized. Unfortunately it could be the case of concrete-like materials.

Besides, it can be stated that in the context of FFM the two PMs are just an approximation of the LMs.

2.3 Coupled stress and energy FFM

According to the introduced criteria, internal lenghts Δ_{LS} and Δ_{LE} are considered and to obtain their values the contemporaneus fulfilment of the two limit cases (long crack failure load for the stress criteria and no crack failure load for the energetic one) has to be imposed. It means that Eq.(2.6) and (2.10) has to be satisfied. Yet it has to be pointed out that the two approaches remains distinct since the achievement of the former implies the violation of the latter and viceversa. In order to bypass this drawback the extension of the crack Δ_{SE} is no more considered as a material constant and becomes a structural parameter. It can be write that:

$$\begin{cases} \int_R^{R+\Delta_{SE}} \sigma_x(y)dy = \sigma_u \Delta_{SE} \\ \int_0^{\Delta_{SE}} G(a)da = G_f \Delta_{SE} \end{cases} \tag{2.13}$$

This implies that the failure happens whenever there is a length Δ_{SE} over which the resultant of stresses is $\sigma_u \Delta_{SE}$ and, at the same time, the energy available for the crack extension is $G_f \Delta_{SE}$. The unkowns of the problems are obviously the failure load σ_f and the critical distance Δ_{SE}.
The fulfilment of the two equations represent a necessary and sufficient condition for the propagation of the crack.
Therefore coupling the stress and energy FFM Eq.(2.13) is obtained and so the present fracture criterion can be called as *coupled FFM criterion*.
The critical length can be evaluated taking into account different rules. In fact it is stated before that there are two stress and two energetic failure criteria so, in this circumstances, at least four combinations are suitable. However the most proper ones concerns the average energy criterion. In a first combination it can be consider that LE approach is coupled to the PS one. In this case the failure can be observed if the stress is higher than the tensile strenght over the crack step Δ and, at the same time, the energy suitable for the crack step has to be equal to the crack extension multiplied by the fracture energy. It means that:

$$\begin{cases} \sigma_x(R+\Delta) = \sigma_u \\ \int_0^{\Delta} G(a)da = G_f \Delta \end{cases} \tag{2.14}$$

Instead if, in a second case, the average stress criterion LS is combined to the LE approach the failure occurs when the stresses resultant over the crack step Δ is equal to

σ_u multiplied by the extension crack lenght Δ. It means that:

$$\begin{cases} \int_R^{R+\Delta_{SE}} \sigma_x(y)dy = \sigma_u \Delta_{SE} \\ \int_0^{\Delta_{SE}} K_I^2(a)da = K_{IC}^2 \Delta_{SE} \end{cases} \tag{2.15}$$

Applying and solving one of these two systems, the conditions for the failure can be predicted that means exctract the values σ_f and Δ. So the approach expressed by (2.14) and (2.15) can be called PS+LE and LS+LE criterion. The first was been introduced by Leguillon (2002) and the secon by Cornetti et al. (2005).

CHAPTER 3

Circular hole in a tensile plate

3.1 Introduction

The investigation of the brittle failure of a plate with a centre circular hole represents a plane problem which was firstly studied by Kirsch in 1898 . Generally, the unkowns in this condition are at least five, the three σ_x, σ_y, τ_{xy} and the two displacements, u and v. In the field of plane elasticity the equations can be reduced to three by considering only σ_x, σ_y e τ_{xy} (regardless the used coordinate system). Indeed, it is possible to impose a unique equation in the unkown ϕ which is a function of the stress components and that gives us the stress field by derivation. It is then possible to obtain the stress field and, obviously, the strain field by the constitutive law and the displacements field by integration. It has to be said that every time that notches or holes are made on a solid body the flow of stress field does not remain uniform. Around the defects, in the case that will be discussed and explained, stresses will attain their maximum value. In case of a hole subjected to a remote uniaxial tensile load it has been demonstrated that this value is equal to three times the nominal one and it decreases moving away from the discontinuity point represented by the hole. Using the Principle of the Superposition of the Effects, it is possible to represent a lot of different situations. In fact it must be noted that in the last fifthy years the world of the Fracture Mechanics was characterized by a continue evolution. Not only the stress field is an important parameter but another one has to be put in evidence, the Stress Intensity Factor. Concerning the SIF, in the Seventies there was a great effort to put together a comprehensive compilation of solutions for cracks available at that time. This was satisfied by Tada's "Stress Analysis of Cracks Handbook" , first out in 1973 and with its third edition published by ASME in which Irwin and Paris cooperated on. According to this handbook not only the Tensile Test but also the Brazilian Test results were compared to the theoretical and numerical ones, (derived from computational analysis) and a characteristic brittle behaviour was delineated. These theoretical studies perfectly explain and are in agreement with the results achieved by the tests conducted and the numerical simulations implemented.

3.2 Kirsch's solution for the stress field

Let us consider an infinite plate subjected to an uniaxial tensile stress σ in the x direction (Fig. 3.1) (Carpinteri, 1992):

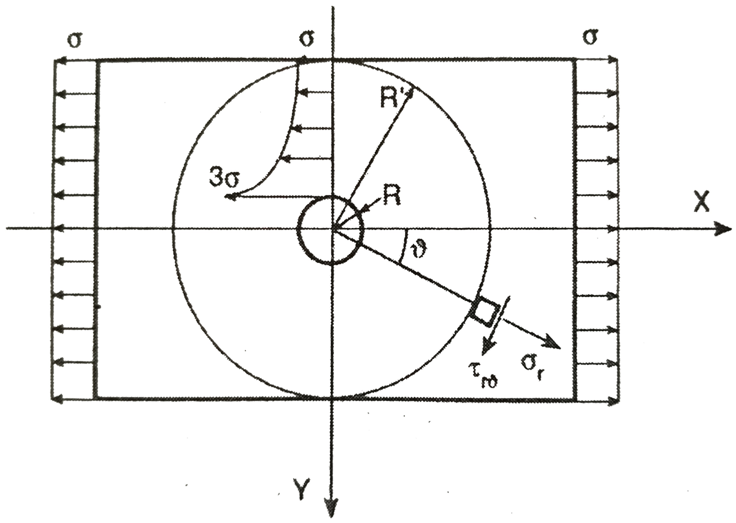

Figure 3.1: Infinite plate subjected to tensile stresses

A circular hole of radius R is present at the center of the plate. Let us fix a polar coordinate system (R', θ), where R' is the radial coordinate and θ is the circumferential one. On the body σ_θ , σ_r and $\tau_{r\theta}$ are present. No other external stresses wil act on the hole and, therefore, only the two stresses, σ_r and $\tau_{r\theta}$ will act. The distribution of stresses is perturbed in the surroundings of the hole. The aim is to calculate the effect of stress concentration on the edge of the defect.

Let us consider the portion of the plate inside the circumference of radius R', where $R' >> R$.

The external circumference has a radius *R'* that tends to infinite and conditions will have to be put (that will not be polar symmetric conditions) on it. Then Mohr relations will have to be applied to express the boundary conditions in polar coordinates. The boundary conditions at the infinite are not trivial because they are not axisymmetric; we will have an uniaxial stress with center on σ_r axis and that is tangent to the $\tau_{r\theta}$ axis. Then the center will have (σ/2, 0) coordinates.
Accordingly stresses acting upon the external circumference are not perturbed by the hole. They can be deduced from the Mohr's Circle. Let us consider a vector ray that runs along the circumference of 2θ and length σ/2. This is the representative point of tensions. It can be obtained:

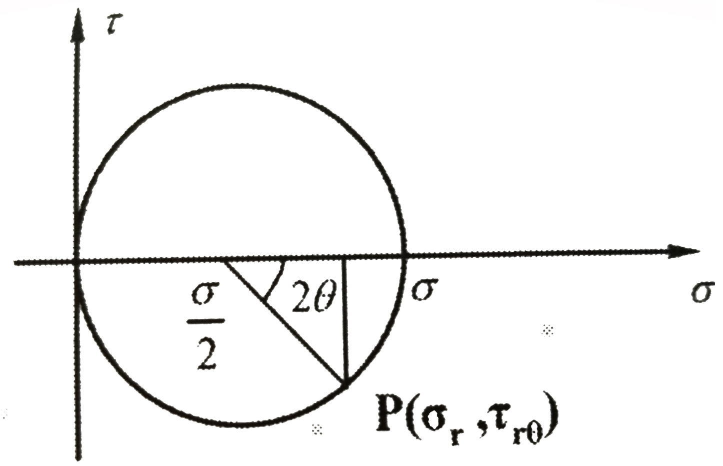

Figure 3.2: Mohr's Circle

$$\sigma_r(r = R') = \frac{1}{2}\sigma\,(1 + \cos 2\theta) \qquad abscissa\ of\ the\ representative\ point \tag{3.1}$$

$$\tau_{r\theta}(r = R') = -\frac{1}{2}\sigma \sin 2\theta \qquad ordinate\ of\ the\ representative\ point \tag{3.2}$$

Basically these are the boundary conditions. The radial stress (3.1) is made of two parts. The first component is constant and provides the following stress field within the ring:

$$\sigma_r = -\frac{\sigma}{2}\frac{R^2 R'^2}{R'^2 - R^2}\frac{1}{r^2} + \frac{\sigma}{2}\frac{R'^2}{R'^2 - R^2} \tag{3.3}$$

$$\sigma_\theta = +\frac{\sigma}{2}\frac{R^2 R'^2}{R'^2 - R^2}\frac{1}{r^2} + \frac{\sigma}{2}\frac{R'^2}{R'^2 - R^2} \tag{3.4}$$

In the limit case in which *R'* $\rightarrow \infty$ (the case of a circulare hole in an infinite means) the two expressions simpifly as follows:

$$\sigma_r = -\frac{\sigma}{2}\left(1 - \frac{R^2}{r^2}\right) \tag{3.5}$$

$$\sigma_\theta = \frac{\sigma}{2}\left(1 + \frac{R^2}{r^2}\right) \tag{3.6}$$

The second component of σ_r (3.1) and the tangential stress $\tau_{r\theta}$ (3.2) provide a stress field which can be evaluated starting from the Airy function expressed below:

$$\phi = f(r)\cos 2\theta \tag{3.7}$$

Equation (3.7) gives us the actual solution that satisfies the boundary conditions.
By imposing the operator ∇^4 to the Airy function the θ variable can be removed and we have:

$$\left(\frac{d^2}{dr^2} + \frac{1}{r}\frac{d}{dr} - \frac{4}{r^2}\right)^2 f = 0 \tag{3.8}$$

In this way *f* represents the only unkown of the problem.
The complete integral of Eq.(3.8) is:

$$f(r) = Ar^2 + Br^4 + \frac{C}{r^2} + D \tag{3.9}$$

Obviously, we have a complete integral that is function of four arbitrary constants because we have a fourth order operator.
The stress field components are obtained by derivation of the Airy stress function:

$$\sigma_r = -\left(2A + \frac{6C}{r^4} + 4Dr^2\right)\cos 2\theta \tag{3.10}$$

$$\sigma_\theta = \left(2A + 12Br^2 + \frac{6C}{r^4}\right)\cos 2\theta \tag{3.11}$$

$$\tau_{r\theta} = \left(2A + 6Br^2 - \frac{6C}{r^4} - \frac{2D}{r^2}\right)\sin 2\theta \tag{3.12}$$

The indetermination of the constants can be solved imposing the boundary conditions. Two of them will be imposed on the infinite edge and the other two on the edge of the hole:

$$\sigma_r(R') = \frac{\sigma}{2}\cos 2\theta \tag{3.13}$$

$$\tau_{r\theta}(R') = -\frac{\sigma}{2}\sin 2\theta \tag{3.14}$$

The polarsymmetric solution will be added to Eq.(3.13) and (3.14) at the end.

$$\sigma_r(R) = 0 \tag{3.15}$$

$$\tau_{r\theta}(R) = 0 \tag{3.16}$$

There are no normal and tangential stresses. Composing the two ones it will be stated that the stress vector is zero.
Equations (3.13), (3.14), (3.15), (3.16) form a system of four equations in four unkowns. Introducing them in the expressions of the stress field (3.10), (3.11), (3.12) it ca be obtained:

$$2A + \frac{6C}{R'^4} + \frac{4D}{R'^2} = -\frac{\sigma}{2} \tag{3.17}$$

$$2A + 6BR'^2 - \frac{6C}{R'^4} - \frac{2D}{R'^2} = -\frac{\sigma}{2} \tag{3.18}$$

$$2A + \frac{6C}{R^4} + \frac{4D}{R^2} = 0 \tag{3.19}$$

$$2A + 6BR^2 - \frac{6C}{R^4} - \frac{2D}{R^2} = 0 \tag{3.20}$$

For *R'* $\rightarrow \infty$ the above expressions simplify as follow:

$$A = -\frac{\sigma}{4}, \qquad B = 0, \qquad C = -\frac{\sigma}{4}R^4, \qquad D = \frac{\sigma}{2}R^2 \tag{3.21}$$

Introducing the four constants (3.21) into Equations (3.10), (3.11) and (3.12) and adding the polarsymmetric solution yields:

$$\sigma_r = \frac{\sigma}{2}\left(1 - \frac{R^2}{r^2}\right) + \frac{\sigma}{2}\left(1 + 3\frac{R^4}{r^4} - 4\frac{R^2}{r^2}\right)\cos 2\theta \tag{3.22}$$

$$\sigma_\theta = \frac{\sigma}{2}\left(1 + \frac{R^2}{r^2}\right) - \frac{\sigma}{2}\left(1 + 3\frac{R^4}{r^4}\right)\cos 2\theta \tag{3.23}$$

$$\tau_{r\theta} = -\frac{\sigma}{2}\left(1 - 3\frac{R^4}{r^4} + 2\frac{R^2}{r^2}\right)\sin 2\theta \tag{3.24}$$

The foundamental parameters of the study are only two: the nominal stress σ applied at infinite and the radius *R* of the hole. In fact, if *R'* $\to \infty$ the two equations on the edge are verified while for *R'=R* the two equations on the hole are obtained.
Considering the three components of the stress field, talking about resistence verifications, the circumferential component σ_θ is that on which we have to focus on, also because is the tensile tension of the hole that, in certain points, assumes the maximun value (a symmetric one on the intersection points of the vertical symmetric axis and the circumference of the hole) as it can be seen in the figure:

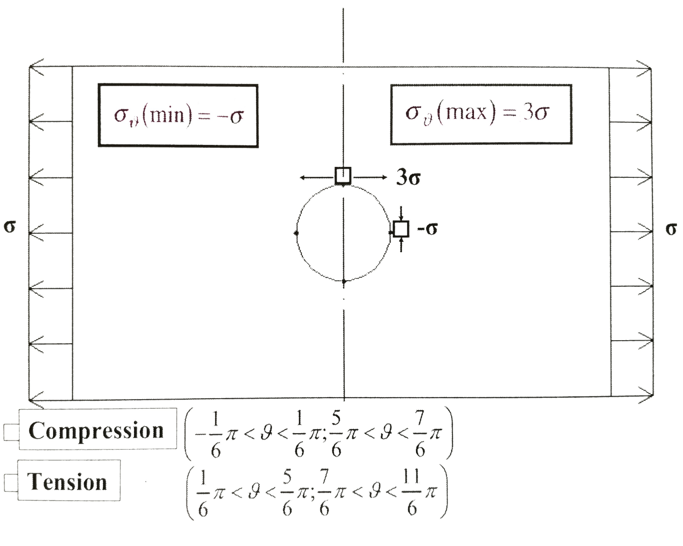

Figure 3.3: Properties of the solution

So for $\theta = \frac{\pi}{2}$ we have :

$\sigma_\theta(\max) = 3\sigma$ and $\sigma_\theta(\min) = -\sigma$

The function shuts off quite rapidly and it can be confused with the asymptotic value provided by the nominal stress at a distance equal to three or four times the radius from the center. The concentration factor, equal to three in this case, is a multiplier of the stresses, it does not depend from the radius of the hole and it is fundamental in terms of verification. Therefore it is evident the local character of the stress concentration around the hole:

If r increases σ_θ tends quickly to σ
At a distance:

- r=2R and $\theta = \frac{\pi}{2}$

$$\sigma_\theta = \frac{\sigma}{2}\left(1 + \frac{R^2}{4R^2}\right) - \frac{\sigma}{2}\left(1 + 3\frac{R^4}{16R^4}\right)(-1) = 1.22\sigma \tag{3.25}$$

- r=4R and $\theta = \frac{\pi}{2}$

$$\sigma_\theta = \frac{\sigma}{2}\left(1 + \frac{R^2}{16R^2}\right) - \frac{\sigma}{2}\left(1 + 3\frac{R^4}{256R^4}\right)(-1) = 1.04\sigma \tag{3.26}$$

It is true that removing some of the material a weakness is created but it can be said that the smaller is the radius of the hole the greater is the concentration of stresses. It can be seen as a kind of compensation.
In this case of study was analyzed only the infinite plate subjected to an uniaxial stress but different loads, tensile and compressive ones, can be applied. Thanks to the elasticity the solution can be reached through the Superposition of the Effects. For example, composing vertical tensile stress with a horizontal one it will be find an isotropic and hydrostatic state of stress. The Mohr Circle is reduced to a point with a concentration factor of the stresses equal to two (due to a factor equal to three and a factor equal to minus one) as it can be seen below:

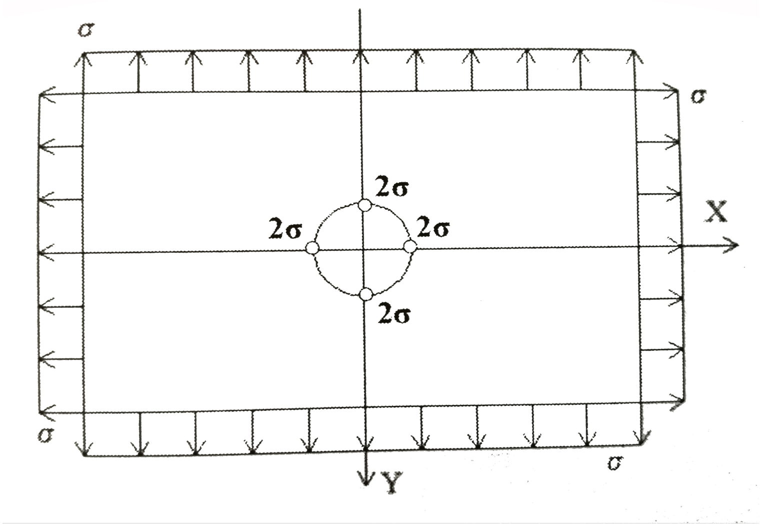

Figure 3.4: Superposition of effects

This case is a polarsymmetric one.
When the boundary condition is uniform at infinity the circumferential stress is also uniform on the edge of the hole.
Composing, instead, a compressive vertical stress with a tensile horizontal one the following case can be found and so on:

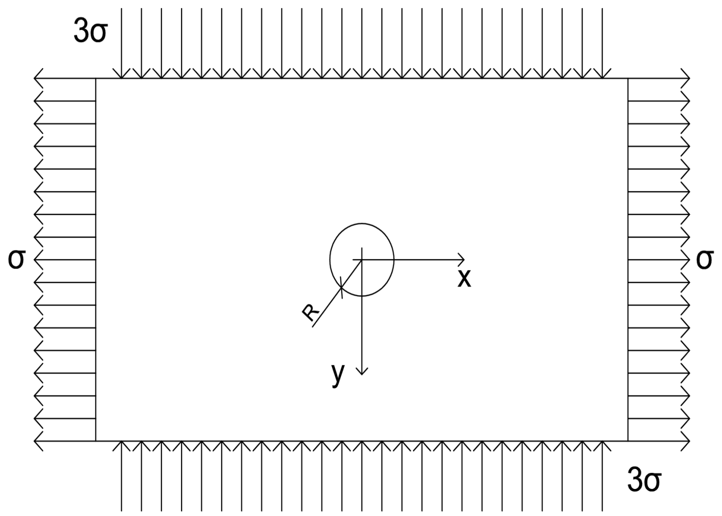

Figure 3.5: Superposition of effects

Substituting in the Eq.(3.23) the new conditions, the following equation is obtained:

$$\sigma_\theta = \sigma_\theta(\pi/2) + 3\sigma_\theta(0) = \sigma\left(1 - \frac{R^2}{r^2} + 6\frac{R^4}{r^4}\right) \tag{3.27}$$

3.3 Tada's solution for the stress intensity factor

A fundamental subsequent step is the evaluation of the Stress Intensity Factor (SIF) that represents the multiplier of the stress field in the surroundings of the damage (the hole in this case) in a structural body. Obviously, it has to be underlined that this is possible, because we are in the field of the plane stresses. For the settled purpose different paths can be traced. Close-form solutions (but these are limited to very simple case), Computational solutions and Experimental solutions (that will be the argument of the next section) and the use of Fracture Handbook. It was already found out how the stress concentration factor at the edge of a hole is independent from the hole radius but the size of the stress concentration region depends on *R*. The expression for the stress intensity factor of two symmetric cracks emanating from a circular hole in an infinite rectangular plate in tension can be searched out in the Tada's work, named "The Stress Analysis Of Cracks Handbook". In fact as it can be seen:

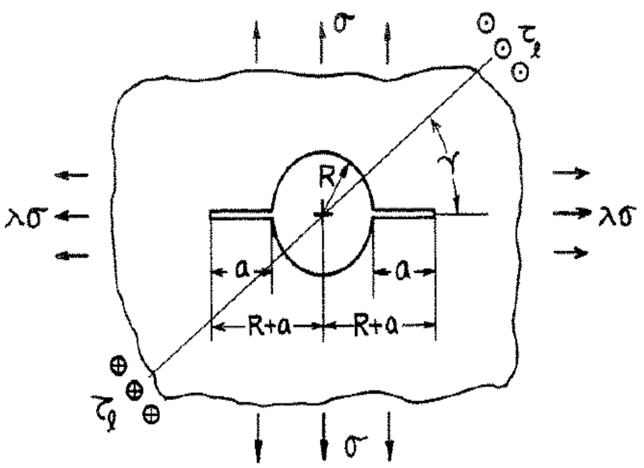

Figure 3.6: Infinite plate with two symmetric cracks

The equations that allow to obtain the SIF values can be summarize below:

$$K_I(a) = \sigma\sqrt{\pi a}F_\lambda(s) \tag{3.28}$$

$$s = \frac{a}{R+a} \tag{3.29}$$

$$F_\lambda(s) = (1 - \lambda)F_0(s) + \lambda F_1(s) \tag{3.30}$$

$$F_0(s) = 0.5(3 - s)[1 + 1.243(1 - s)^3] \tag{3.31}$$

$$F_1(s) = 1 + (1 - s)[0.5 + 0.743(1 - s)^2] \tag{3.32}$$

These formulas have been applied for different situations, varying the characteristic parameters λ (to take into account both tensile and compressive load case), the radius of the hole *R* and the crack extension length *a*, in order to achieve the values of the SIF for five different hole dimensions inside a plate, subjected to a compressive force, and again for others five different hole dimensions inside a plate subjected, instead, to a tensile force.
The following tables show the SIF results of a plate with a hole at its center considering two different values of the hole radius, respectively 4 mm and 0.5 mm and an extension of the cracked region *a* which varies from 0.1 mm and 0.8 mm.

- For the compressive load case, assuming λ = -3 the trend can be represented as follows: :

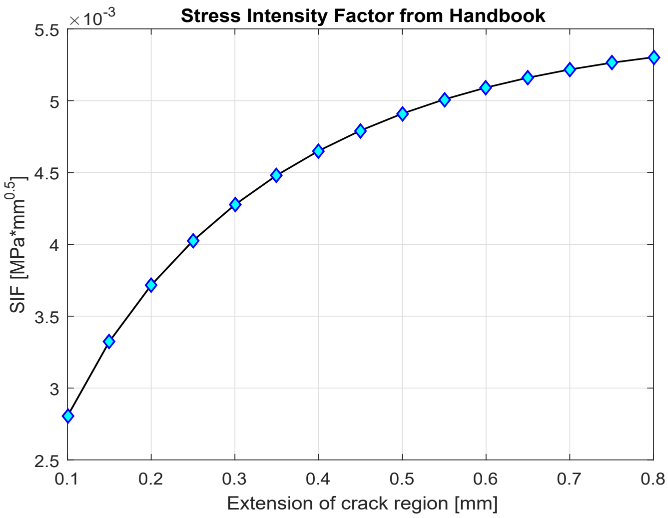

Figure 3.7: SIFs $R = 4$mm

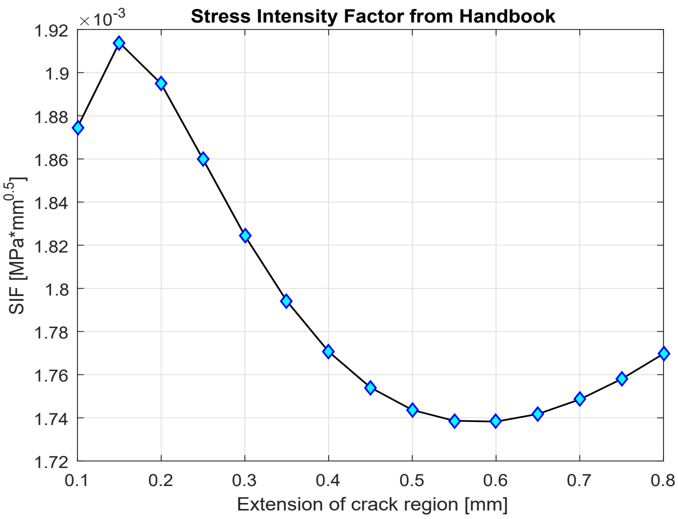

Figure 3.8: SIFs R=0.5mm

- For the tensile load case, assuming $\lambda = 0$ the trend can be represented as follows: :

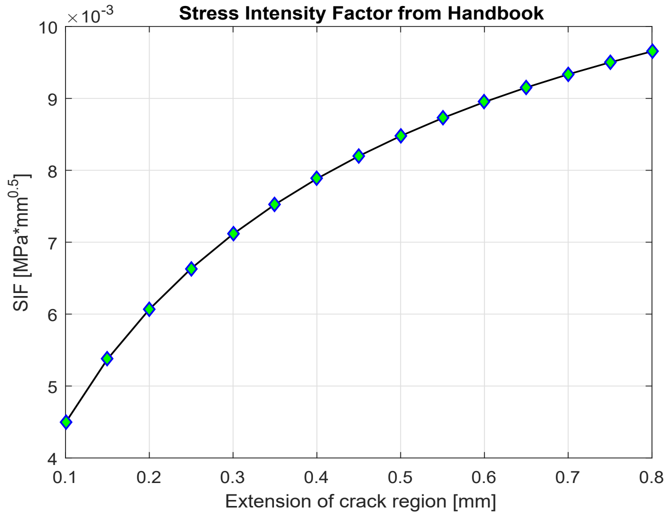

Figure 3.9: SIFs $R = 4$mm

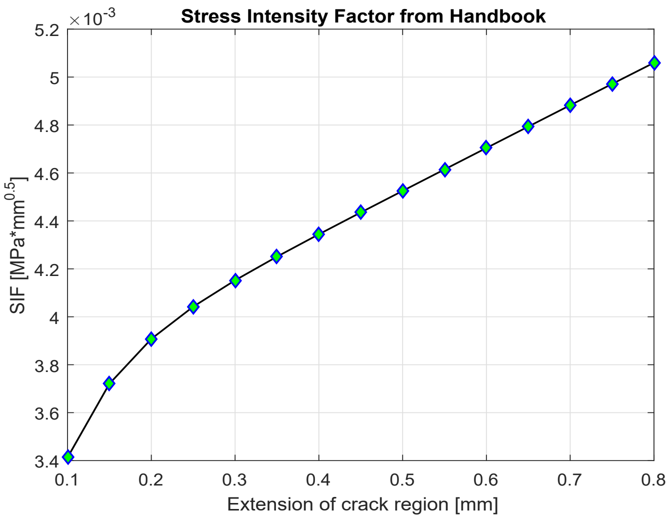

Figure 3.10: SIFs R=0.5mm

As it can be seen the properties of the material do not get involved in the computations of the SIFs (no material characteristic appears in the formulations), therefore the results are generally applicable whatever is the constituent material of the bodies under analysis. From the graphics two different trends can be observed, both for the compressive and tensile load case. The first is a growing monotonous trend shown in correspondence of relatively large diameter hole as it can be seen in Fig.(3.5) and (3.9). Differently the presence of small diameter hole in the plate produces a downward trend concerning the compressive case as shown in Fig. (3.10). A peak is evident in correspondence of an extension of the crack equal to 0.15 mm and then a plunge untill an extension of the crack region of about 0.6 mm. Afterwards, again, a soft increment of the SIF can be noticed. Instead, this behavior is not exhibited in the tensed plate with small radius hole. In fact, in Fig.(3.10), after a cracked region of about 0.2 mm, almost a linear trend can be pointed out. The different conducts can be justified taking into account that in presence of so small defect dimensions, phenomena of plasticization may occur.

3.4 Computational analysis

The target of the study is, now, the application of the Finite Element Method (FEM) to analyze the brittle behavior of finite dimensions plates with center circular hole. In order to do this the ANSYS® Software is used (software developed by EnginSoft©). In particular, for this field of study, ANSYS Mechanical APDL is the most appropriate product of those available. The structural integrity of a component under the action of applied loads and environmental conditions can be examined thanks to this branch of the software. Indeed, fracture mechanics uses concepts from applied mechanics to develop an understanding of the stress and deformation fields around a crack tip when a crack is present in a structure. A sound knowledge of these stress and deformation fields helps in developing fail-safe and safe-life designs for structures. Such fracture-mechanics-based design concepts are, now, widely used. So the circular plate subjected to compressive load and the rectangular plate subjected to tensile load are implemented. Two different materials are used for all geometries, PolyMethylMethAcrylate (PMMA) and GeneralPurposePolyStyrene (GPPS). In sake of simplicity only two models for each load case are described.

3.4.1 Brazilian Disk geometry

The study is focused on the circular plate. It exhibits a radius of 40 mm and a thickness of 10 mm. To simplify, the modeling is however conducted in a 2D field and then, the results are multiplied by the value of the thickness. This parameter is different for PMMA and GPPS models, respectively 10 mm and 8 mm. In the first case the hole radius is equal to 4 mm and in the second one to 0.5 mm. The first step (and the fundamental one) concerns the choice of the type of element. It has a great importance especially about the crack-tip region. In fact, because high stress gradients exist in the region around the crack tip, the finite element modeling of a component containing a crack requires special attention in that region. The recommended element type for a 2-D fracture model is PLANE183, the 8-node quadratic solid:

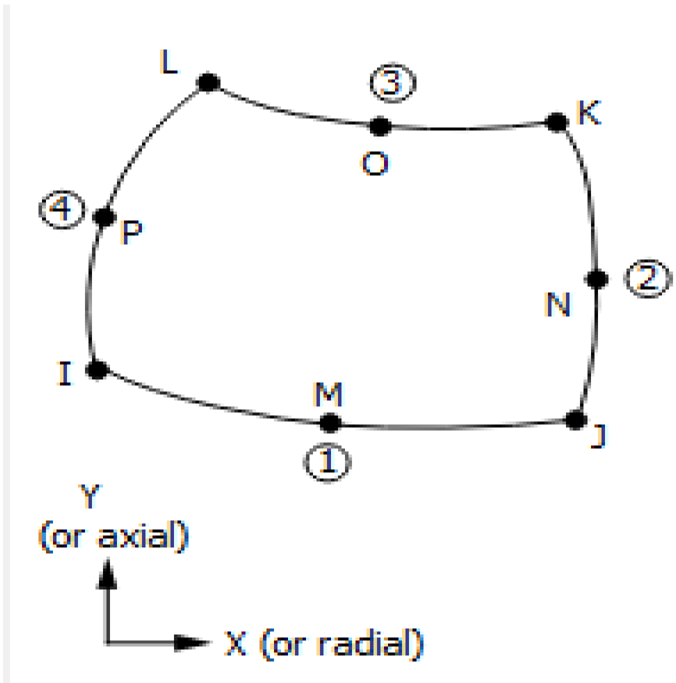

Figure 3.11: 8-node element

So, as it can be seen in Fig.(3.13):

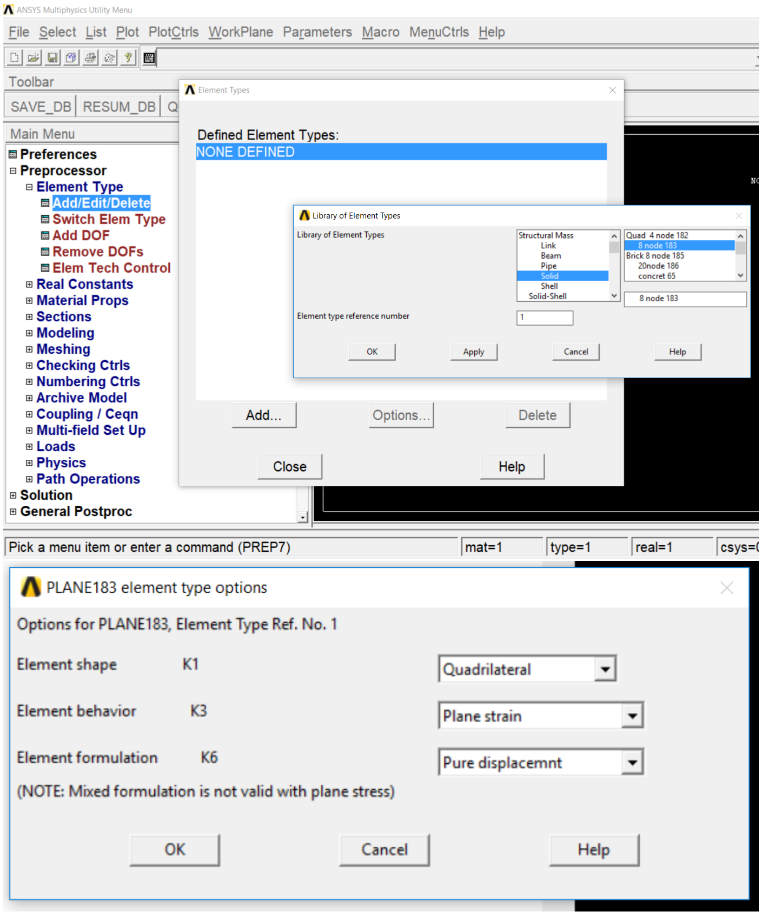

Figure 3.12: ANSYS element choice and characteristic

PLANE183 has quadratic displacement behavior and is well suited to modeling irregular meshes. KEYOPT(3) is used to enable generalized plane strain. It is possible, then, to describe the characteristics of the materials through the material models present in the library. In particular the structural model is chosen (linear-elastic-isotropic). The Young Modulus and the Poisson Coefficient are inserted. It must be remembered that Mechanical APDL does not work with specific unit of measure so any input must be consistent with the measurement unit of the desired results. Hence, considering PMMA, an E = 2960 MPa and a ν=0.38 are entered:

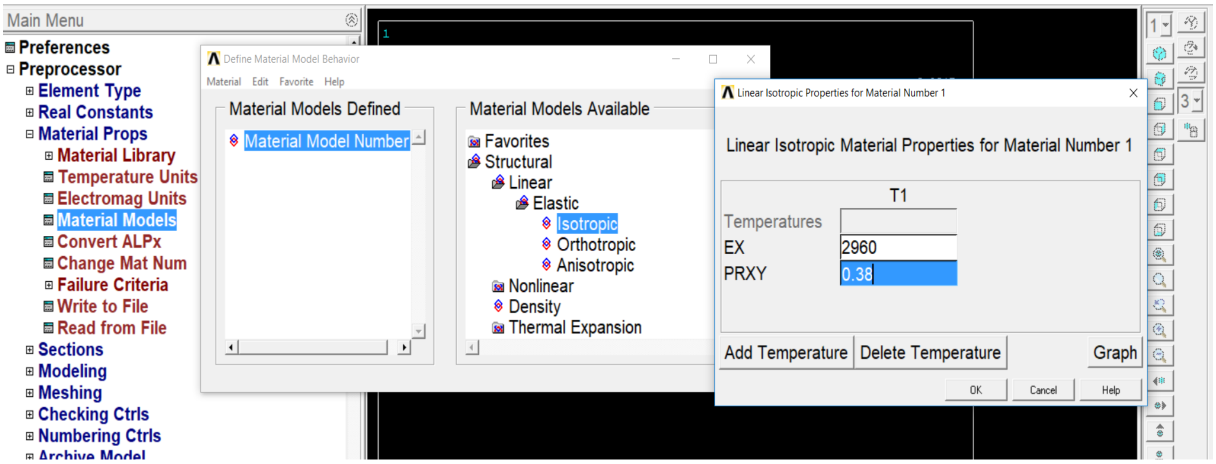

Figure 3.13: Material Model

Instead, when the models refer to GPPS, an E = 3100 MPa and a ν=0.34 are imposed. Once these preliminar steps are concluded, the geometry can be shaped. Due to the symmetry of the problem (geometric and load symmetry) only a quarter of the disk is analyzed. Several ways can be adopted for this purpose. In this case it is convenient to create several keypoints in active coordinate system and then the lines and arcs of the disk. Afterwards the create areas operation can be done. In this way the crack tip can be assigned as the origin of the coordinate system. Obviously, at this stage of modeling also the extension of the crack region has to be expressed. Considering an a = 0.4 mm Tab.(3.1) and (3.2) are used:

KEYPOINT	x[mm]	y[mm]
6	0	0
5	0	-0.4
1	0	-4.4
4	0	35.6
2	4.0	-4.4
3	40.0	-4.4

Table 3.1: KPs coordinates - $R = 4$ mm

KEYPOINT	x[mm]	y[mm]
6	0	0
5	0	-0.4
1	0	-0.9
4	0	39.1
2	0.5	-0.9
3	40.0	-0.9

Table 3.2: KPs coordinates - $R = 0.5$ mm

So the geometries in Fig.(3.14) and (3.15) are:

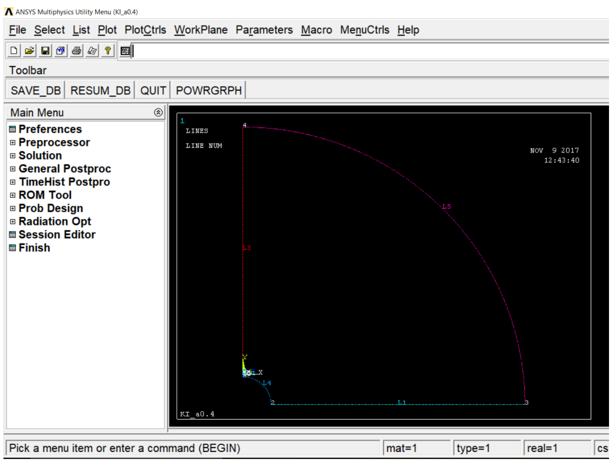

Figure 3.14: Brazilian Disk Geometry - $R = 4$ mm

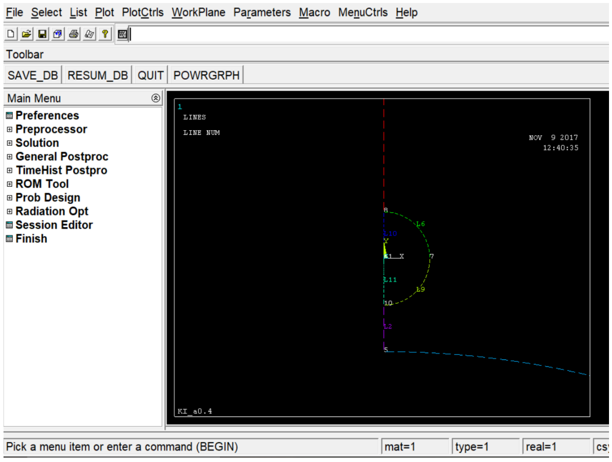

Figure 3.15: Zoom to the crack-tip - $R = 4$ mm

The same can be observed for the small radius hole:

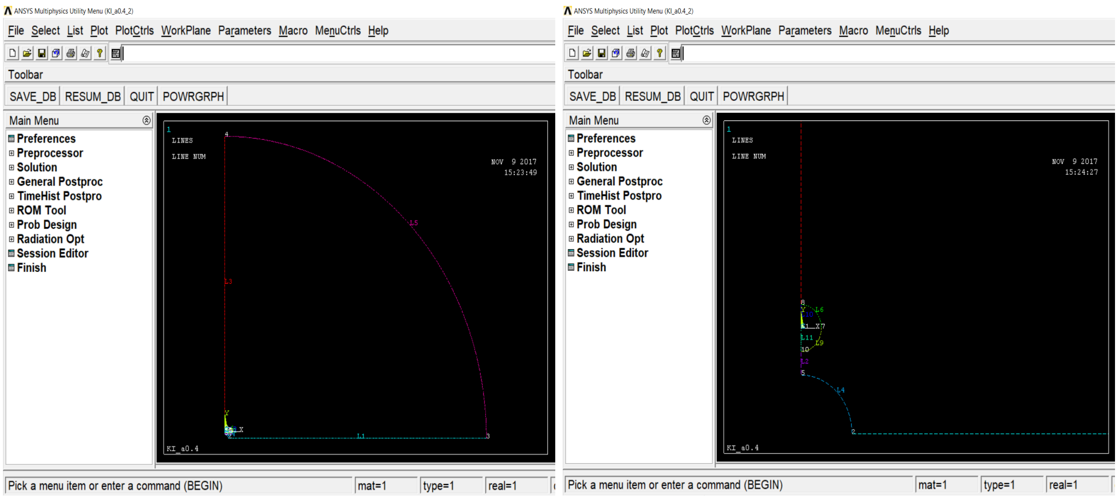

Figure 3.16: Brazilian Disk Geometry - $R = 0.5$ mm

The subsequent step is of extreme importance to achieve a good result in the numerical simulation and it is the meshing of the areas and, above all, of the crack region. It has to be emphasized that the meshing has to be different respectively if only the stresses have to be evaluated or if the SIFs have to be calculated. In the first case an almost ordinary mesh can be realized. So not too extreme refinement is needed and the simple mesh tool can be used. Different is the situation in the second case. Indeed, the crack-tip has to be created. This can be done through the Concentrat KPs Tool in Size Cntrls as shown in Fig.(3.17):

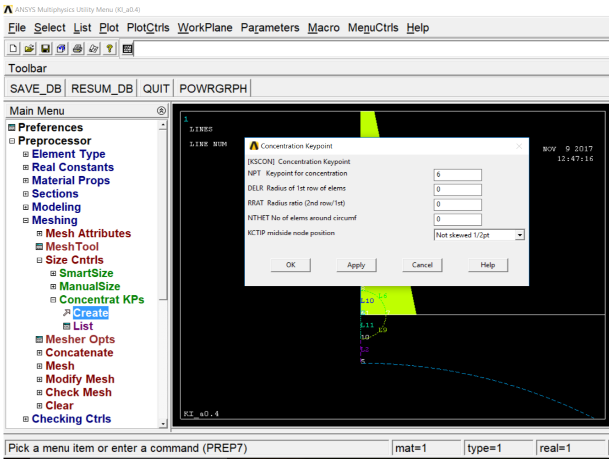

Figure 3.17: Concentrat KPs Tool

The precise nature of stress and deformation fields depends on the material, geometry and other factors. To capture the rapidly varying stress and deformation fields,a refined mesh has to be used in the region around the crack tip. For linear elastic problems, the displacements near the crack tip vary as $\sqrt{r}$ where r is the distance from the crack tip. The stresses and strains are singular at the crack tip, varying as $\frac{1}{\sqrt{r}}$. To produce this singularity in stresses and strains, the crack tip mesh has to provide crack faces coincident and quadratic elements, around the crack tip, with the midside nodes placed at the quarter points (singular elements) as shown below:

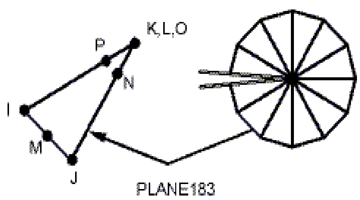

Figure 3.18: Singular Element

So the first row of elements around the crack tip should be singular. The Concentrat KPs Tool assigns element division sizes around a keypoint. It automatically generates singular elements around the specified keypoint (the keypoint 6 in this case). Other fields on the command allow to control the radius of the first row of elements and the number of elements in the circumferential direction. For reasonable results, the first row of elements around the crack tip should have a radius very small. In the circumferential direction, roughly one element every 30° or 40° is recommended so 8 elements are imposed. The crack-tip elements should not be distorted and should take the shape of isosceles triangles. The meshes implemented are displayed in Fig.(3.19) and (3.20):

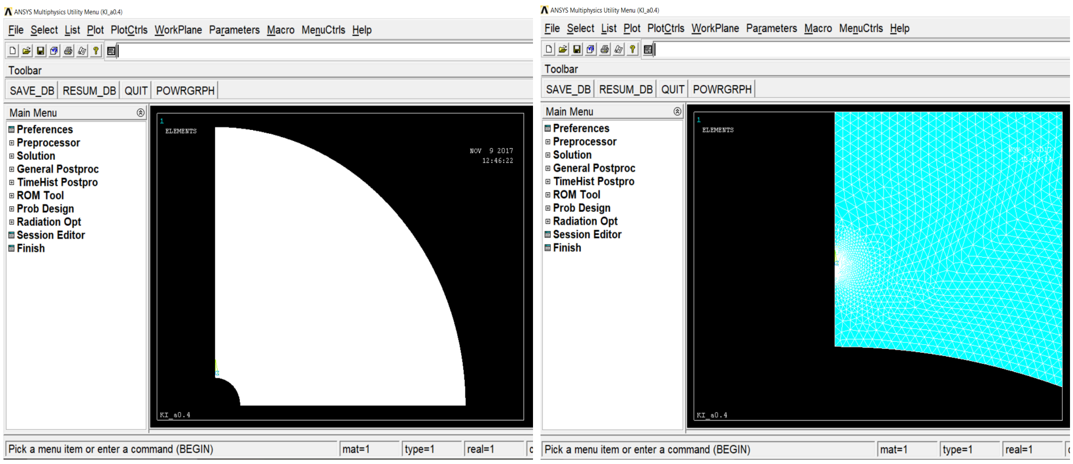

Figure 3.19: General mesh and mesh around the crack-tip - $R = 4$ mm

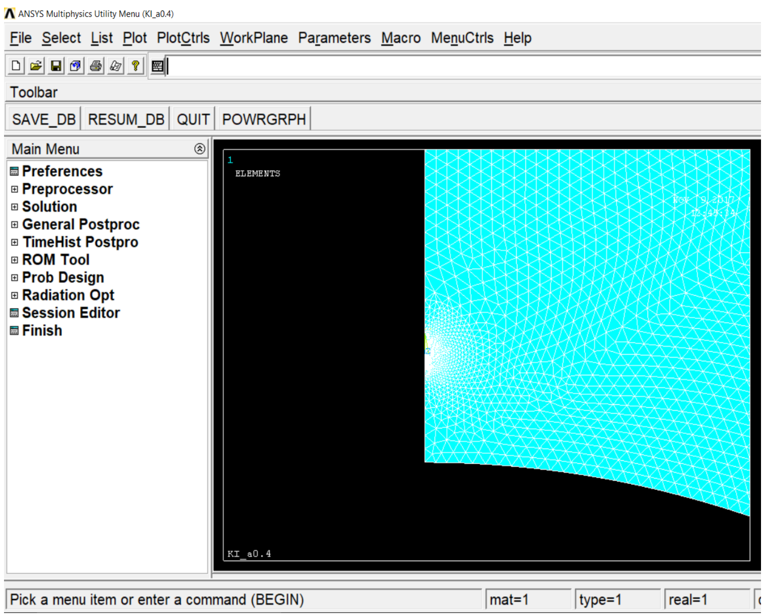

Figure 3.20: Mesh around the crack-tip - $R = 0.5$ mm

Made the mesh it is necessary to give the boundary conditions input to the software and to apply the load. Due to the presence of a quarter model the symmetric boundary conditions can be selected and, for the external load, a concentrated force in y direction equal to -0.5 N is selected. The force is applied in correspondence of the keypoint 4 in this case so at the top of the vertical radius of the disk:

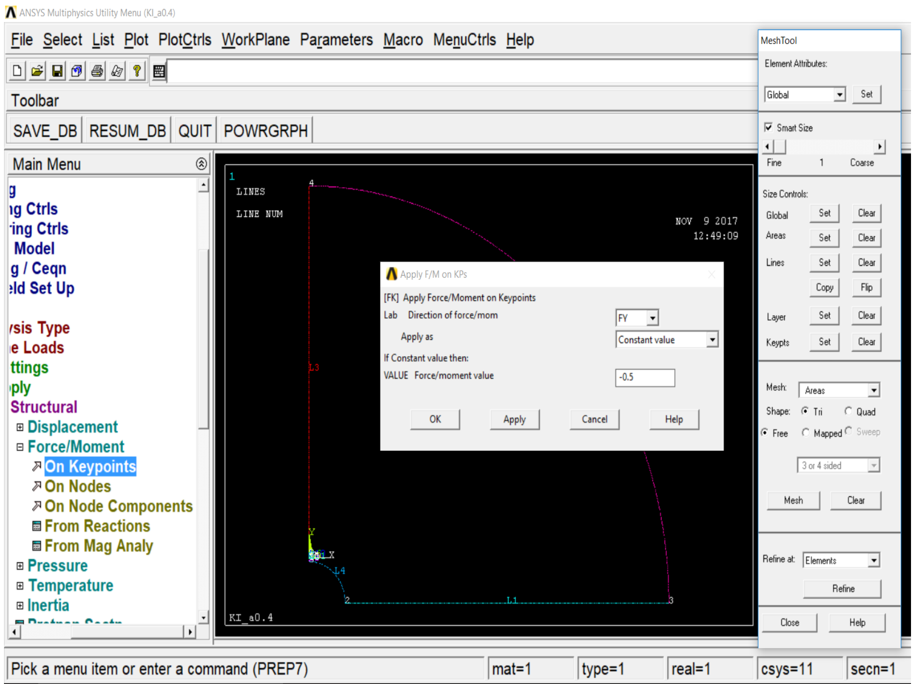

Figure 3.21: Application of the load

The phase of the preprocessing is thus concluded. It is, hence, possible to solve the problem and to extract the results. So stresses and SIFs are evaluated. In particular, the stress field has to be calculated along the crack face. To obtain it a path along the vertical radius has to be described. In the postprocessing selecting the two keypoints 1 e 4 the path can be created with the specific tool and the stress output extrapolated as below:

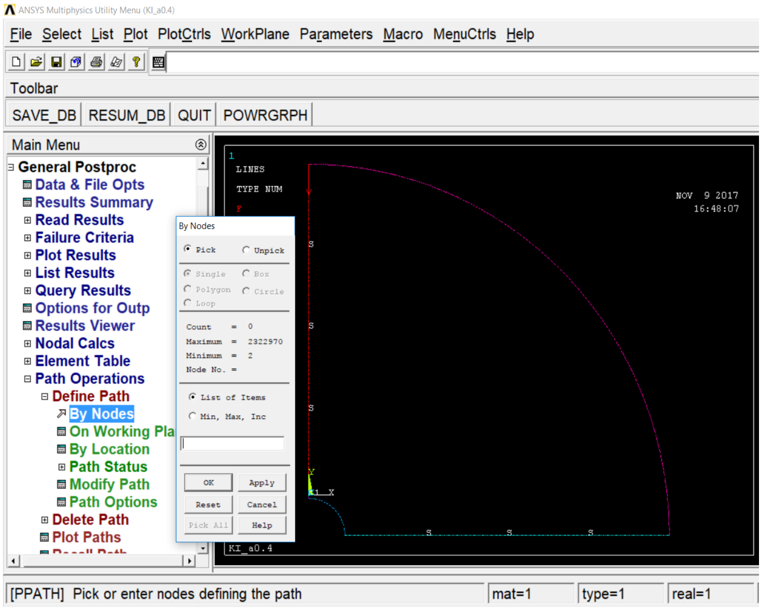

Figure 3.22: Path definition

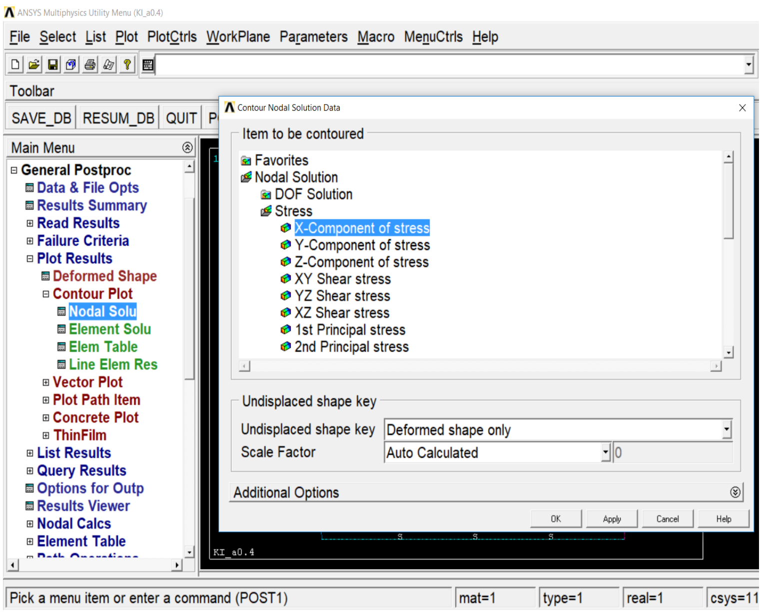

Figure 3.23: Stress output

Different is the situation for the calculus of the SIFs. In particular the crack-tip node component and the crack-extension direction are both necessary for the stress-intensity factors calculation. The auxiliary crack-tip field is based on the crack-extension direction. To ensure the accuracy of the SIFs calculation, it is crucial that it is correctly defined the crack-extension. The auxiliary crack-tip field is based, besides, on the local crack-tip coordinate systems. So in the postprocessing phase, first of all, a local coordinate system, has to be created. This can be done selecting the crack-tip as first node (it represents the origin of the coordinate system), a whatever second node along the crack face and a third node orthogonal to the last one. In this way local crack-tip coordinate system shows the local x-axis pointed to the crack extension and the local y-axis pointed to the normal of the crack surfaces or edges. The program automatically calculate the local coordinate systems based on the input crack front nodes and the normal of the crack surface or extension directions. Activated the local coordinate system it has to be specified that the SIFs results has to be evaluated considering this specific system. Then, again a path has to be imposed. For 2-D crack geometry, firstly the crack-tip node has to be selected. For a half-crack model, two additional nodes are required, both along the crack face. The second node has to be close to the crack tip and the third one a little further away (it can be picked the first three nodes) as indicated in Fig.(3.24):

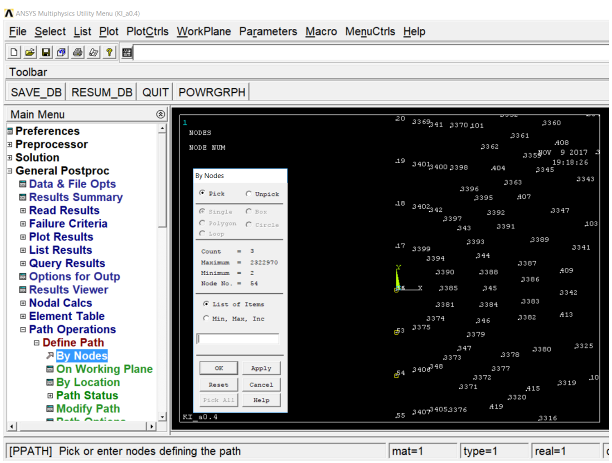

Figure 3.24: Definition of the Path for the evaluation of the SIFs

Finally, with the Nodal Calcs Tool the SIFs can be extracted. The command specifies whether the model is plane-strain or plane-stress. The asymptotic or near-crack-tip behavior of stress is usually thought to be that of plane strain. The KCSYM field specifies whether the model is a half-crack model with symmetry boundary conditions, a half-crack model with antisymmetry boundary conditions, or a full-crack model; it can be seen below:

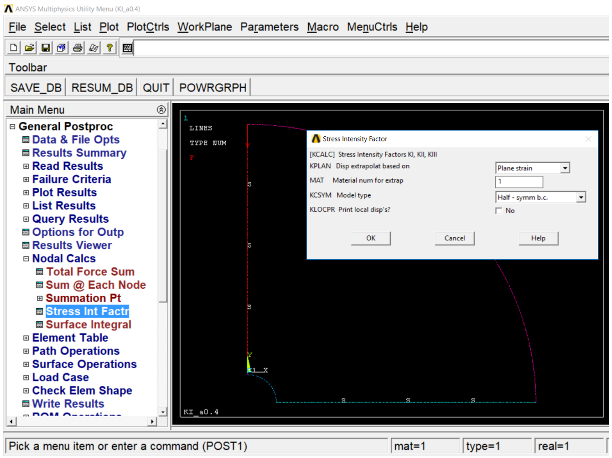

Figure 3.25: Nodal Calcs Tool

In the Tab.(3.3) and (3.4) are provided the SIFs of the numerical simulations of the two hole diameters in correspondence of the different extension of the crack region with the attached errors compared to the theoretical values:

a[mm]	$\mathrm{K_I(a)E-2[MPa\cdot mm^{0.5}]}$	e[%]
0.1	0.0283	0.9689
0.15	0.0335	0.7325
0.2	0.0373	0.4553
0.25	0.0404	0.4703
0.3	0.0430	0.5147
0.35	0.0451	0.5922
0.4	0.0471	1.3606
0.45	0.0483	0.7839
0.5	0.0499	1.5160
0.55	0.0509	1.6676
0.6	0.0521	2.2976
0.65	0.0527	2.0505
0.7	0.0519	-0.5459
0.75	0.0528	0.2731
0.8	0.0536	1.0308

Table 3.3: SIFs values and errors - R = 4 mm

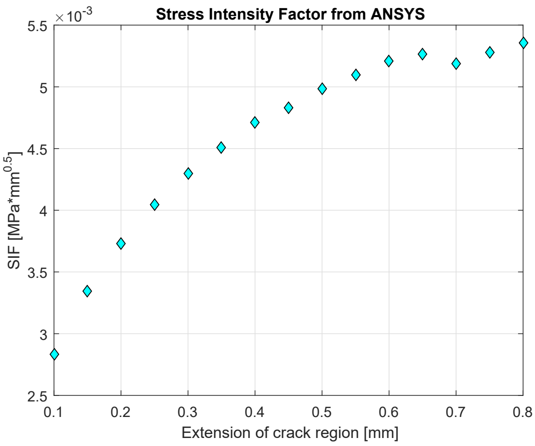

Figure 3.26: SIFs - R = 4 mm

a[mm]	$\mathrm{K_I(a)E-2[MPa \cdot mm^{0.5}]}$	e[%]
0.1	0.01862	-0.70578
0.15	0.01932	0.92654
0.2	0.01873	-1.15377
0.25	0.01851	-0.49201
0.3	0.01836	0.61656
0.35	0.01786	-0.44401
0.4	0.01767	-0.18562
0.45	0.01739	-0.88268
0.5	0.01752	0.46086
0.55	0.01736	-0.12826
0.6	0.01725	-0.79136
0.65	0.01750	0.46526
0.7	0.01741	-0.41459
0.75	0.01765	0.36928
0.8	0.01755	-0.86590

Table 3.4: SIFs values and errors - R = 0.5 mm

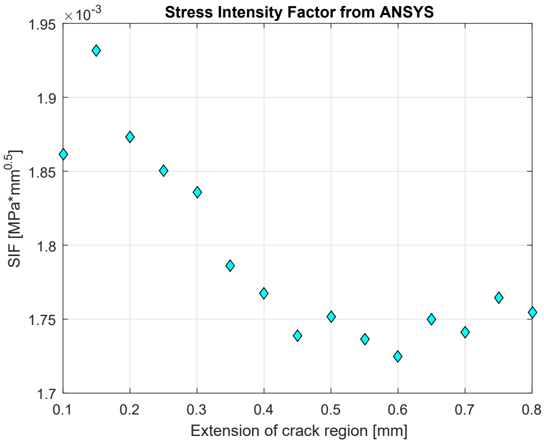

Figure 3.27: SIFs - R = 0.5 mm

As it can be easily deduced from the previous results, the numerical simulations of the Brazilian Disks produces values in perfect agreement with the theoretical studies. The biggest mistakes, in terms of SIFs, are found in correspondence of circular plate with the bigger radius with a maximum value almost equal to 2.30% which is, however, an acceptable value.

3.4.2 Tensile plate geometry

In this second part the numerical simulations of the rectangulare plate with circular hole are described. The plate is characterized by a lenght l= 100 mm and a height h= 40 mm. Also in this case the computational analysis is conducted in a 2D field and then the results are multiplied by the thickness. The constituent materials are PMMA and GPPS and the respectevely thicknesses are equal to 10 mm and 8 mm. Two cases are examined, the first considering a hole radius equal to 4 mm and the second one with a hole radius equal to 0.5 mm. In sake of simplicity only an extension of the crack region a = 0.4 mm, for each geometry, is shown. As for the Brazilian Disk, the first step is the choice of the element. Obviously, also for this case, the element which has to be used is the PLANE 183 and the element behavior selected is the plane strain. The Young modulus and Poisson coefficient are entered once selected the Material Props Tool and isotropic linear elastic type, among the structural models, is chosen. To create the geometries the keypoints coordinates are inserted in the active coordinate system as shown in Table (3.5) and (3.6):

KEYPOINT	***x*[mm]**	***y*[mm]**
7	0	0
3	0	-15.6
2	0	0.4
1	0	4.4
6	4.0	4.4
5	50.0	4.4
4	50.0	-15.6

Table 3.5: KPs coordinates - R = 4 mm

KEYPOINT	***x*[mm]**	***y*[mm]**
7	0	0
3	0	-19.1
2	0	0.4
1	0	0.9
6	4.0	0.9
5	50.0	0.9
4	50.0	-19.1

Table 3.6: KPs coordinates - R = 0.5 mm

As it can be seen in the figures below only a quarter of the plates are modeled thanks to the geometric and load symmetry of the cases:

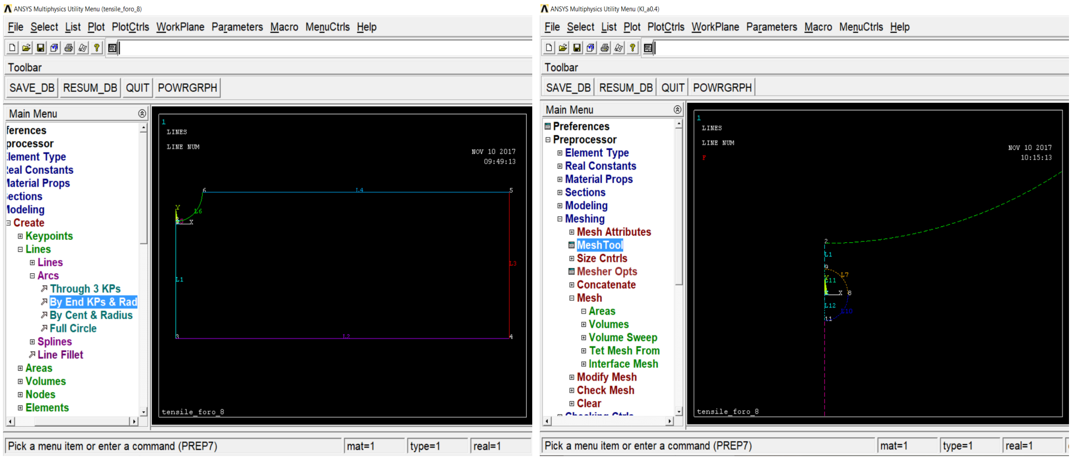

Figure 3.28: Rectangular plate - $R = 4$ mm

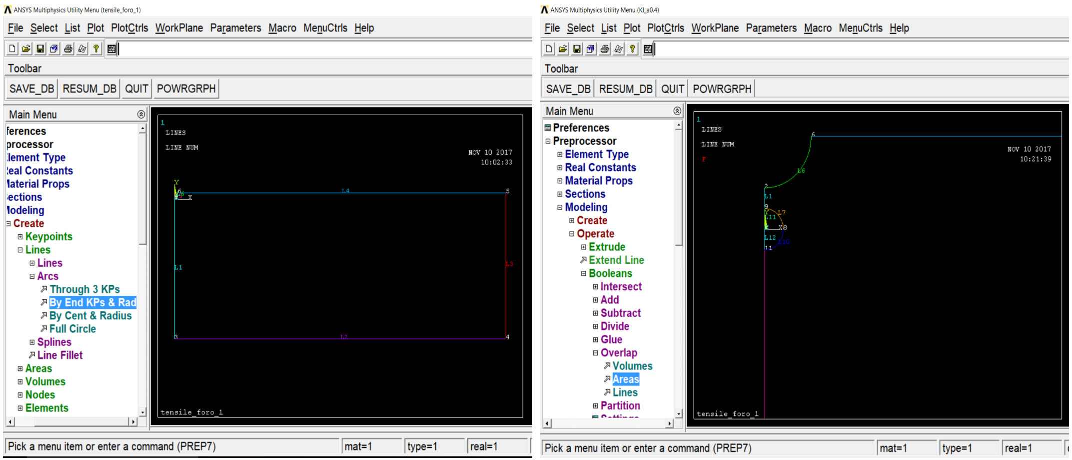

Figure 3.29: Rectangular plate - $R = 0.5$ mm

It is necessary, then, to create the mesh. For what concern the evaluation of the stresses along the crack face a not too much refined mesh is needed. It can be performed with triangular elements. Instead for the calculation of the SIFs the crack-tip has to be delineated in Size Cntrls Tool considering a very small first row of elements around the crack-tip value and a number of elements again equal to 8. The crack-tip elements should assume a not distorted isosceles triangular shape. The meshes implemented are shown in Fig.(3.30) and (3.31):

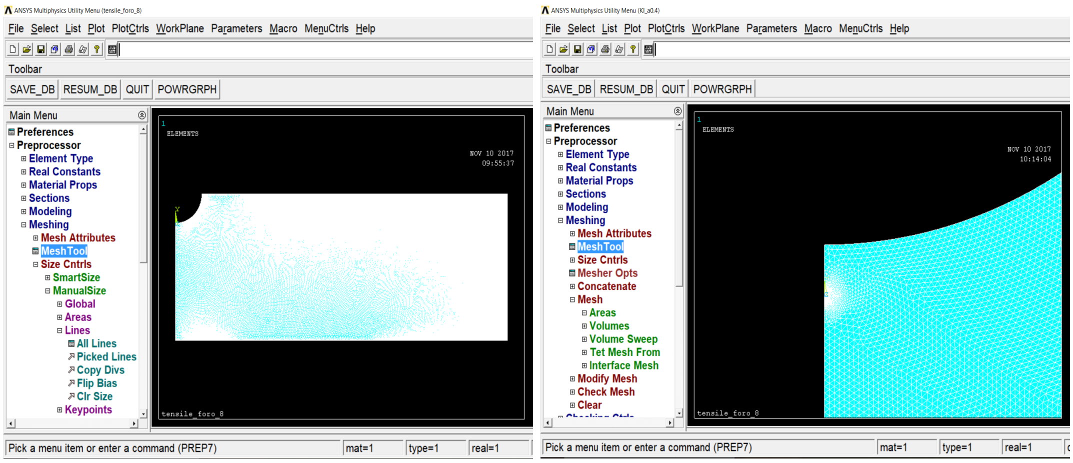

Figure 3.30: Rectangular plate mesh - R = 4 mm

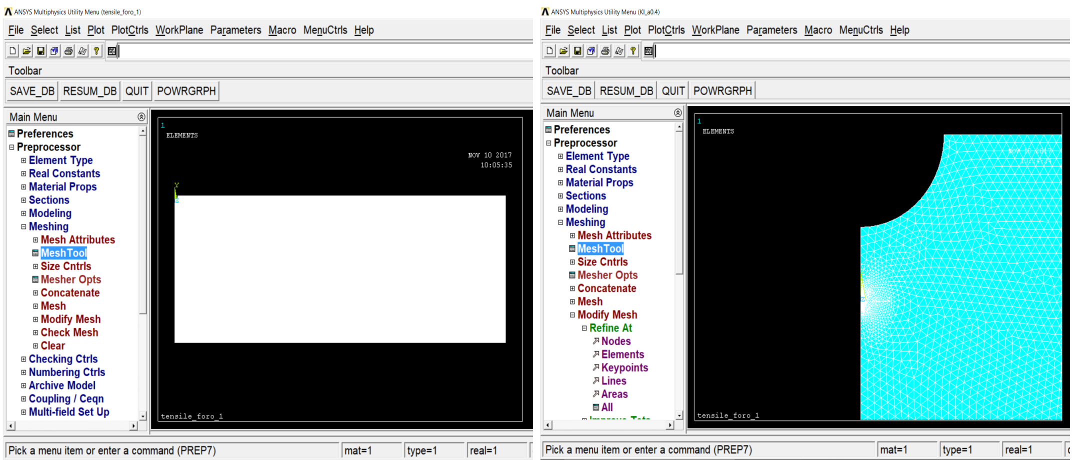

Figure 3.31: Rectangular plate mesh - R = 0.5 mm

Before to run the analysis the symmetric boundary conditions have to be applied and the tensile concentrated force equal to 0.5 N has to be put on the correspondent keypoint (the number 5 in this cases):

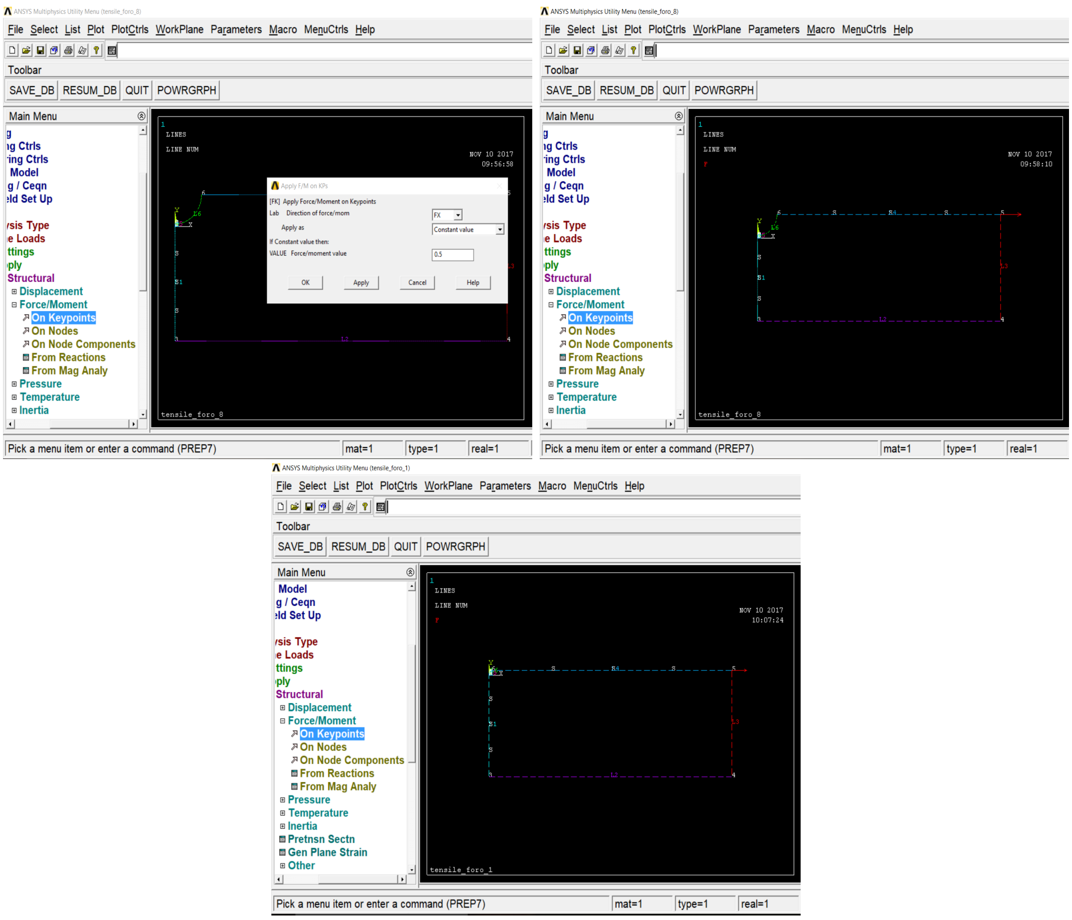

Figure 3.32: Rectangular plate load - R = 4 mm and R = 0.5 mm

Afterwards the models can be solved. For what concern the stress field, a path has to be indicated. It has to be realized picking the nodes along the failure direction. A local coordinate system, then, has to be created. The origin is selected in correspondence of the crack-tip. Then a node along the propagation of the crack has to be picked and, at the end, a node in the orthogonal direction. This new coordinate system has to be chosen to be the active one. In the general postprocessing the path along the extension of the crack is delineated and the SIFs are extracted. The values and the correlated percentage of error compared to the theoretical results for the two cases are provided in Tab(3.7) and (3.8):

a[mm]	$\mathbf{K_I(a)E-2[MPa\cdot mm^{0.5}]}$	$\mathbf{e[\%]}$
0.1	0.004493	0.041341644
0.15	0.0054	0.482497952
0.2	0.0061	0.551340332
0.25	0.0067	0.975560746
0.3	0.00718	0.922257402
0.35	0.0076	0.984157164
0.4	0.00795	0.840210396
0.45	0.00826	0.751424103
0.5	0.00856	0.970523171
0.55	0.00879	0.728661058
0.6	0.00901	0.670840722
0.65	0.00919	0.420138033
0.7	0.0094	0.697631023
0.75	0.00956	0.615908904
0.8	0.009713	0.61218595

Table 3.7: SIFs values and errors - R = 4 mm

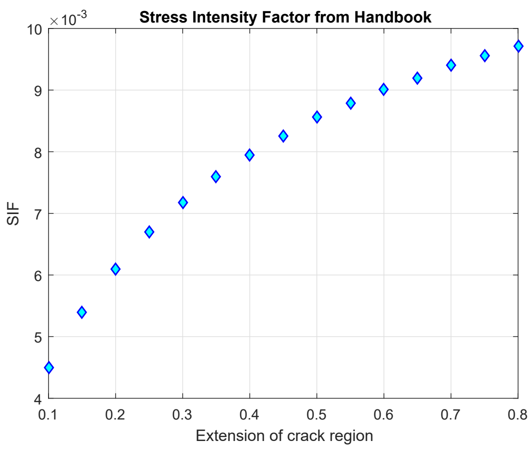

Figure 3.33: SIFs - R = 4 mm

a[mm]	$\mathrm{K_I(a)E-2[MPa \cdot mm^{0.5}]}$	e[%]
0.1	0.00344	0.78368532
0.15	0.00374	0.517541182
0.2	0.00394	0.820614092
0.25	0.00408	0.929655247
0.3	0.00417	0.427639598
0.35	0.0042652	0.336720672
0.4	0.004358905	0.337484745
0.45	0.00447517	0.893820778
0.5	0.004555149	0.658595297
0.55	0.004657393	0.91582858
0.6	0.004745976	0.881102958
0.65	0.004819744	0.545797851
0.7	0.004919252	0.746749651
0.75	0.005003048	0.634472574
0.8	0.005097002	0.731834304

Table 3.8: SIFs values and errors - R = 0.5 mm

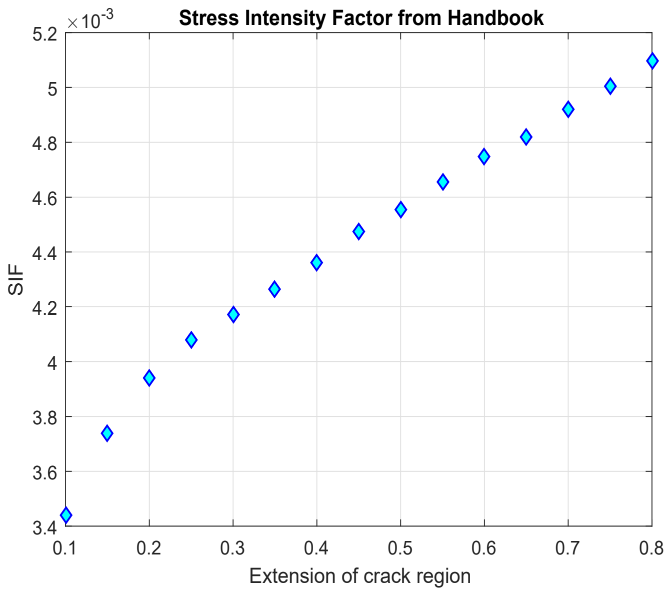

Figure 3.34: SIFs - R = 0.5 mm

As it can be easily seen also in the graphs, the results in case of a rectagular tensed plate with a center hole are almost perfectly in agreement with the theoretical ones. Therefore it can be put in evidence that the numerical simulations can represent a powerful and simple tool to study the brittle behavior of bodies that are affected by defects.

CHAPTER 4

Experimental tests and FFM analysis

4.1 Introduction

Two different types of test were carried out by a team of researchers in Tehran on two different polymeric materials: PMMA and GPPS. The first one is the classical Brazilian Test and the other one is the Tensile Test. The purpose, for both of them, is to investigate size effects, i.e. the decrease of the strength as the hole radius increases and the failure load. Due to their simplicity and efficiency, these tests are very commonly used as testing methods for fracture investigation. This is only one of the many fields in which they are applied (geothecnical, infrastructural and structural ones). Finally, the coupled FFM criterion will be applied to investigate the experimental results.

4.2 Brazilian Disk geometry

The so-called Brazilian Disk or Compression Test has been used for more than fifty years as an indirect method to determine the tensile strength of brittle materials. The method, that has found great application in rock engineering, is now chosen because specimens can be easily prepared and the test is simple to be performed. The test is based on the observation that most brittle materials in biaxial stress fields fail in tension along the loaded diameter of the disc specimen and diametral crack propagation, due to tension, is often observed. In the present study, the diametral crack propagation behaviour in the simple Brazilian Disk is experimentally studied in an attempt to establish a correlation between analitycal studies and invastigated results. For the determination of fracture parameters different typologies of disk specimens are considered, half of them made in PMMA and the other half in GPPS and all of them are characterized by a central hole. So it has been introduced a sort of weakness in the samples.:

Figure 4.1: BD specimen - R = 4 mm

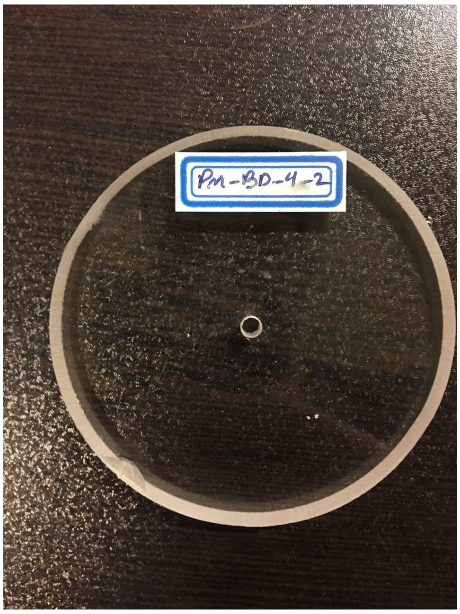

Figure 4.2: BD specimen - R = 2 mm

A disk shaped PMMA specimen is loaded by two steel jaws at diametrically opposite surfaces over an arc of contact of approximately 10 degrees until the failure. Five different radius are used (40 mm, 20 mm, 10 mm, 5 mm and 2.5 mm) and for all the different samples the test is performed three times. The thickness is the same for all of them and it is equal to 10 mm. The radius of the jaws is equal to 1.5 times the radius of the specimens radius. A guide pin clearance permits rotation of one jaw relative to the other. On the other hand, also disk samples of GPPS are tested. There is not only a material difference but also a geometrical parameter, the thickness, is changed. In these cases the thickness is equal to 8 mm. The characteristics of the two polymers are represented in Tab.(4.1):

Material property	**PMMA**	**GPPS**
Tensile strenght [MPa]	78	40
Fracture toughness $[\mathbf{MPa} \cdot \mathbf{m}^{0.5}]$	1.75	0.9

Table 4.1: BD specimens properties

A load is applied through multiple load steps untill the failure as it can be seen in the photos below:

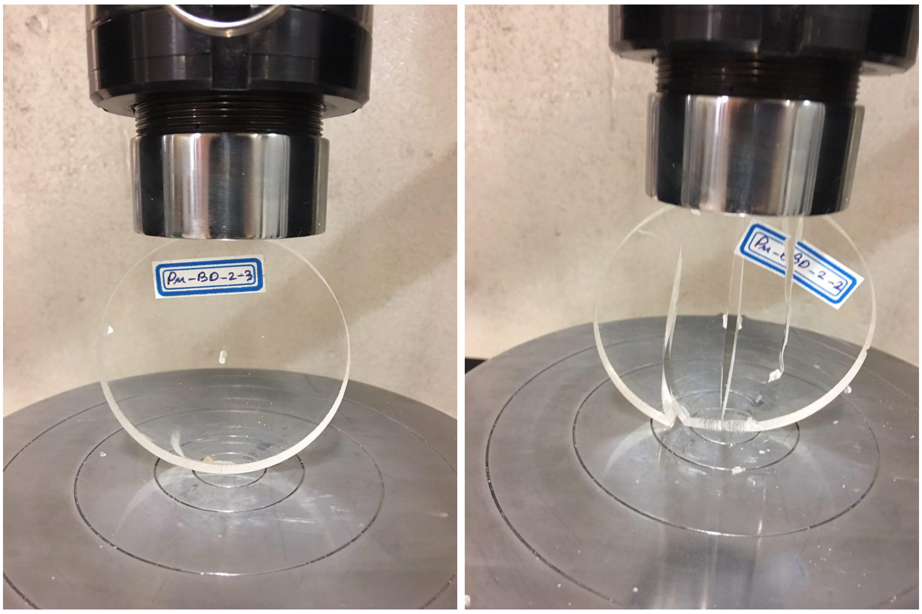

Figure 4.3: BD specimen - R = 1 mm

Three specimens per hole radius are tested and by means of laboratory equipment an average failure load is obtained. The results are shown in Tab.(4.2) and (4.3):

Specimen index	**Fracture load [N]**	**Average load [N]**
P-0.5-1	37150	-
P-0.5-2	33810	35660
P-0.5-3	36020	-
P-1-1	28800	-
P-1-2	26230	27650
P-1-3	27920	-
P-2-1	21830	-
P-2-2	23100	23210
P-2-3	24700	-
P-4-1	20250	-
P-4-2	19936	19420
P-4-3	18074	-
P-8-1	15432	-
P-8-2	16168	15338
P-8-3	14414	-

Table 4.2: BD test results PMMA specimens

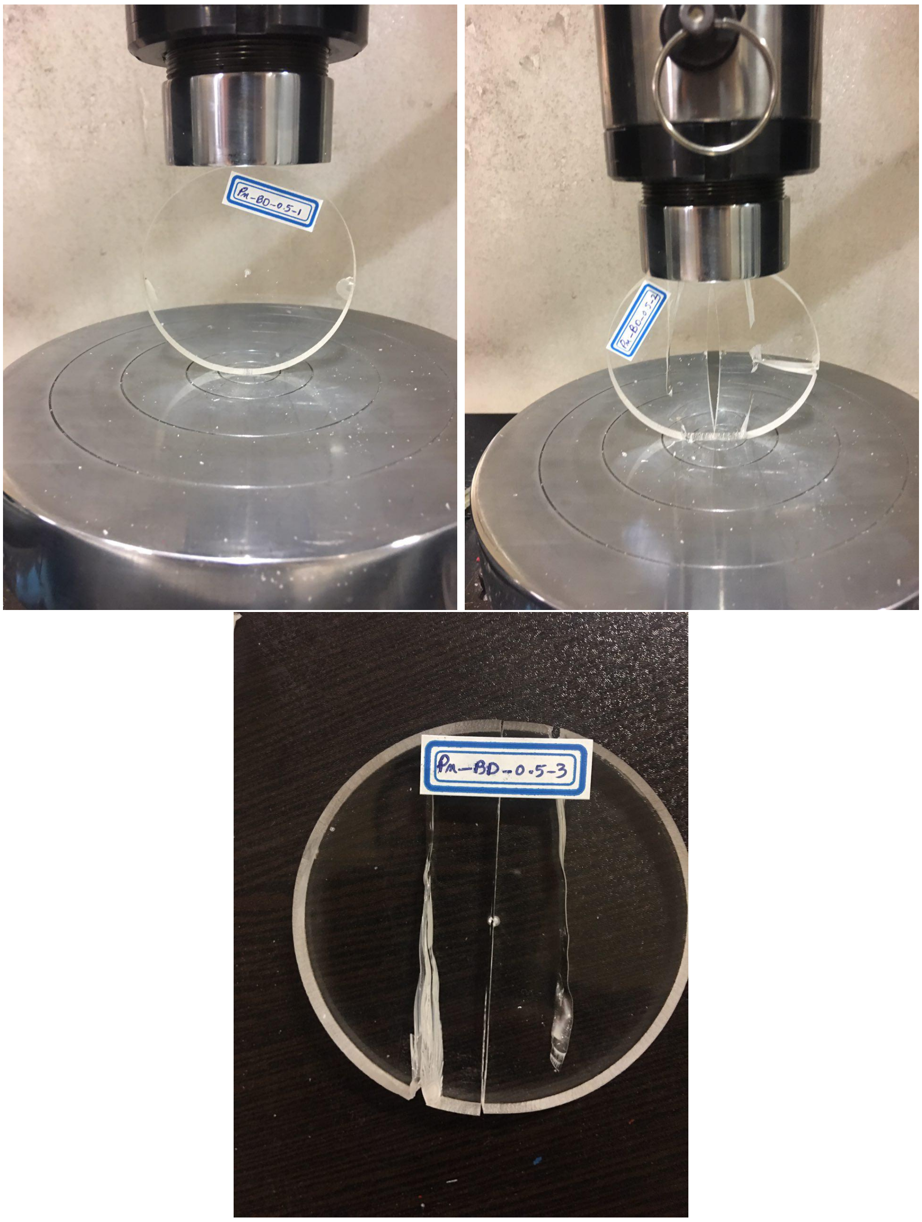

Figure 4.4: BD specimen - $R = 0.25$ mm

Specimen index	Fracture load [N]	Average load [N]
G-0.5-1	15930	-
G-0.5-2	15280	15100
G-0.5-3	14090	-
G-1-1	12260	-
G-1-2	11970	12050
G-1-3	11920	-
G-2-1	9950	-
G-2-2	9130	9360
G-2-3	9000	-
G-4-1	8070	-
G-4-2	7645	7760
G-4-3	7656	-
G-8-1	6525	-
G-8-2	6220	6310
G-8-3	6185	-

Table 4.3: BD test results GPPS specimens

Imposing the FFM theory and applying the Eq.(2.15) is it possible to evaluate numerically the average failure load for each BD.

4.3 Tensile sample geometry

The second tipology of laboratory test conducted to evaluate the failure load is the classical tensile test. The specimens in this case present a rectangular shape and are characterized by a length l = 100 mm and a height h = 40mm. Every specimen show a central hole and different diameter holes are considered. In particular diameters equal to 4 mm, 2 mm, 1 mm and 0.5 mm. For each diameter dimension three specimens are studied. Also for what concern the material of this second kind of samples two different polymers are used, again PMMA and GPPS. The PMMA bodies presents a thickness equal to 10 mm and the GPPS ones a thickness equal to 8 mm. Generally the tensile test is realized on metallic specimens but nowadays this test can be conducted on the most diverse materials (even on concrete like specimens). Indeed, tensile tests are performed for several reasons. The results of tensile tests are used in selecting materials for engineering applications. Tensile properties frequently are included in material specifications to ensure quality. Tensile properties often are measured during development of new materials and processes, so that different materials and processes can be compared. Finally, tensile properties often are used to predict the behavior of a material under forms of loading other than uniaxial tension. The strength of interest may be measured in terms of either the stress necessary to cause appreciable plastic deformation or the maximum stress that the material can withstand. These measures of strength are used, with appropriate caution (in the form of safety factors), in engineering design. Also of interest is the material's ductility, which is a measure of how much it can be deformed before it fractures. Rarely is ductility incorporated directly in design; rather, it is included in material specifications to ensure quality and toughness. Low ductility in a tensile test often is accompanied by low resistance to fracture under other forms of loading. The analyzed specimens can be observe in Fig.(4.5) and (4.6):

Figure 4.5: Tensile test PMMA specimen - R = 2 mm R = 0.25 mm

Figure 4.6: Tensile test GPPS specimen - R = 2 mm

As it can be seen the typical tensile specimen has enlarged ends or shoulders for gripping. The important part of the specimen is the gage section. The cross-sectional area of the gage section is reduced relative to that of the remainder of the specimen so that deformation and failure will be localized in this region. The gage length is the region over which measurements are made and is centered within the reduced section. The distances between the ends of the gage section and the shoulders should be great enough so that the larger ends do not constrain deformation within the gage section. Otherwise, the stress state will be more complex than simple tension. The most important concern inthe selection of a gripping method is to ensure that the specimen can be held at the maximum load without slippage or failure in the grip section. Bending should be minimized. The most common testing machines are universal testers, which test materials in tension, compression, or bending. Testing machines are either electromechanical or hydraulic. The principal difference is the method by which the load is applied. Electromechanical machines are based on a variable-speed electric motor; a gear reduction system; and one, two, or four screws that move the crosshead up or down. This motion loads the specimen in tension or compression. Crosshead speeds can be changed by changing the speed of the motor. A microprocessor-based closed-loop servo system can be implemented to accurately control the speed of the crosshead. Hydraulic testing machines are based on either a single or dual-acting piston that moves the crosshead up or down. In a manually operated machine, the operator adjusts the orifice of a pressure-compensated needle valve to control the rate of loading. In a closed-loop hydraulic servo system, the needle valve is replaced by an electrically operated servo valve for precise control. In general, electromechanical machines are capable of a wider range of test speeds and longer crosshead displacements, whereas hydraulic machines are more cost-effective for generating higher forces. The tensile test involves mounting the specimen in a machine, such as those just described, and subjecting it to tension. The tensile force is recorded as a function of the increase in gage length. It can be observed:

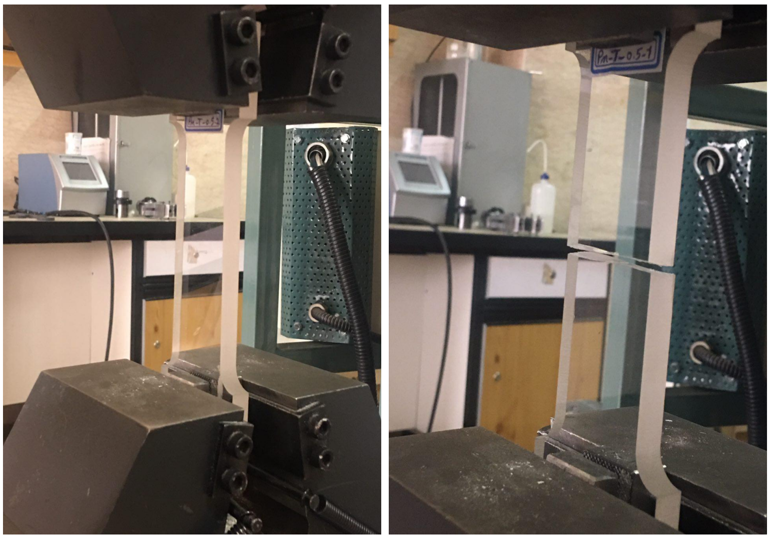

Figure 4.7: Tensile load test PMMA specimen - R = 0.25 mm

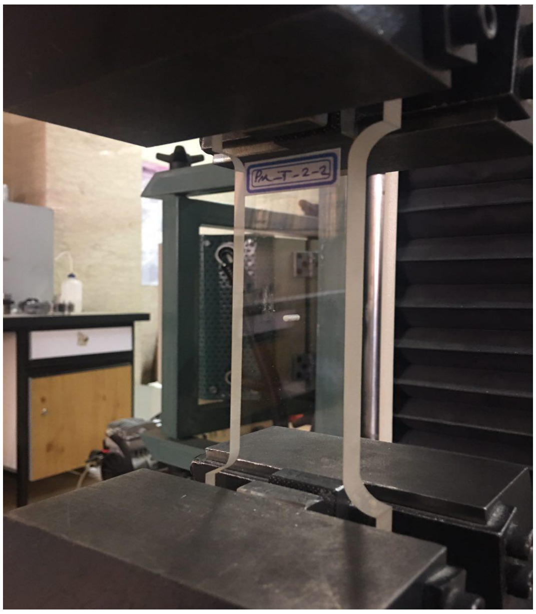

Figure 4.8: Tensile load test PMMA specimen - R = 1 mm

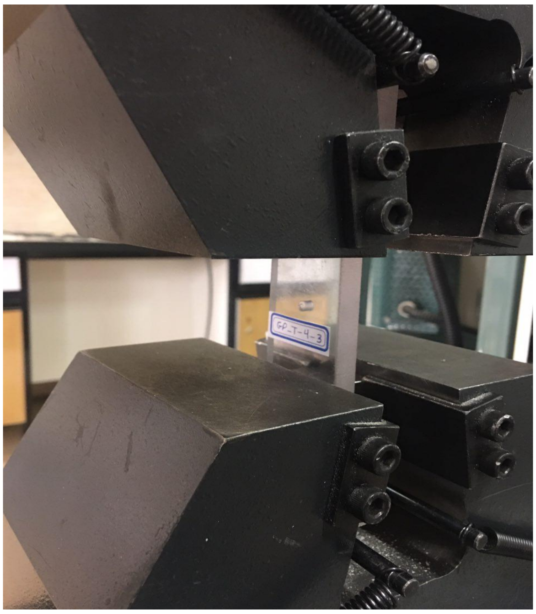

Figure 4.9: Tensile load test GPPS specimen - R = 2 mm

In the simple tensile test, the data comprise a single measurement of peak force and the dimensional measurements taken to determine the cross-sectional area of the test specimen. The first analysis step is to calculate the "tensile strength," defined as the force per unit area required to fracture the specimen. More complicated tests will require more information, which typically takes the form of a graph of force versus extension. Computer-based testing machines can display the graph without paper, and can save the measurements associated with the graph by electronic means. So the tests are performed untill the failure of the specimens. Some broken samples are shown in Fig.(4.10) and (4.11):

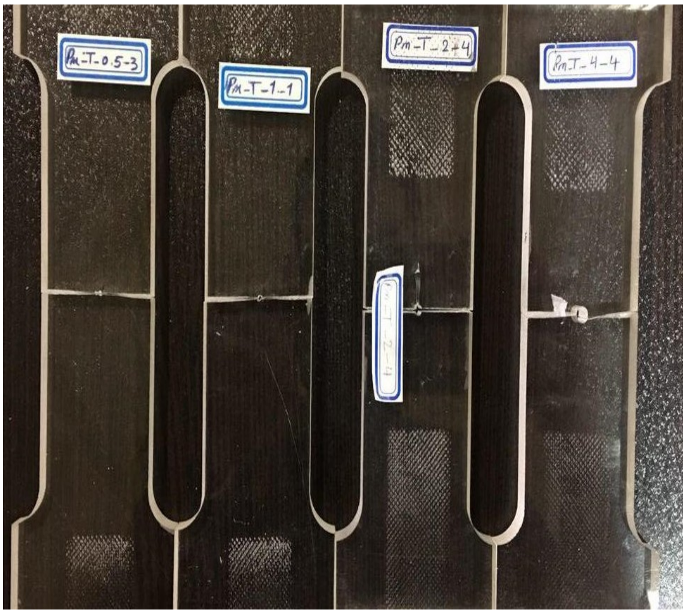

Figure 4.10: PMMA broken specimen

Figure 4.11: GPPS broken specimen

The results are shown in Tab.(4.4) and (4.5):

Specimen index	Fracture load [N]	Average load [N]
P-0.5-1	24100	-
P-0.5-2	21600	22200
P-0.5-3	20900	-
P-1-1	17800	-
P-1-2	17700	17250
P-1-3	16250	-
P-2-1	14900	-
P-2-2	14650	14600
P-2-3	14250	-
P-4-1	11800	-
P-4-2	12250	12200
P-4-3	12550	-

Table 4.4: Tensile test results PMMA specimens

Specimen index	Fracture load [N]	Average load [N]
G-0.5-1	9050	-
G-0.5-2	8580	8730
G-0.5-3	8560	-
G-1-1	7400	-
G-1-2	6900	6950
G-1-3	6550	-
G-2-1	6210	-
G-2-2	5780	5800
G-2-3	5410	-
G-4-1	5250	-
G-4-2	4900	5050
G-4-3	5000	-

Table 4.5: Tensile test results GPPS specimens

Again, applying the FFM theory and with the use of ANSYS® software it is possible to obtain the $P_{critical}$ through the extrapolation of the stress values and the related errors respect the experimental results are evaluated.

4.4 FFM predictions and comparison

After carried out the experimental and numerical tests it can be pointed out the good agreement and the validity of the expressions introduced in chapter 1. The formulae of the LS and LS+LE criteria were particularized to the geometries analyzed. In fact, results provided from the FFM theory compared to the experimental data shows in general a good agreement and the analitical simulations give very close predictions. Anyway some limits can be individuated. The quality of the results is, in fact, related to the geometries of the hole and smaller is the radius of the introduced defects bigger is the percentage of errors in the forecasts of the failure load. It can be seen in the following graphs where the brazilian disk cases are examinated:

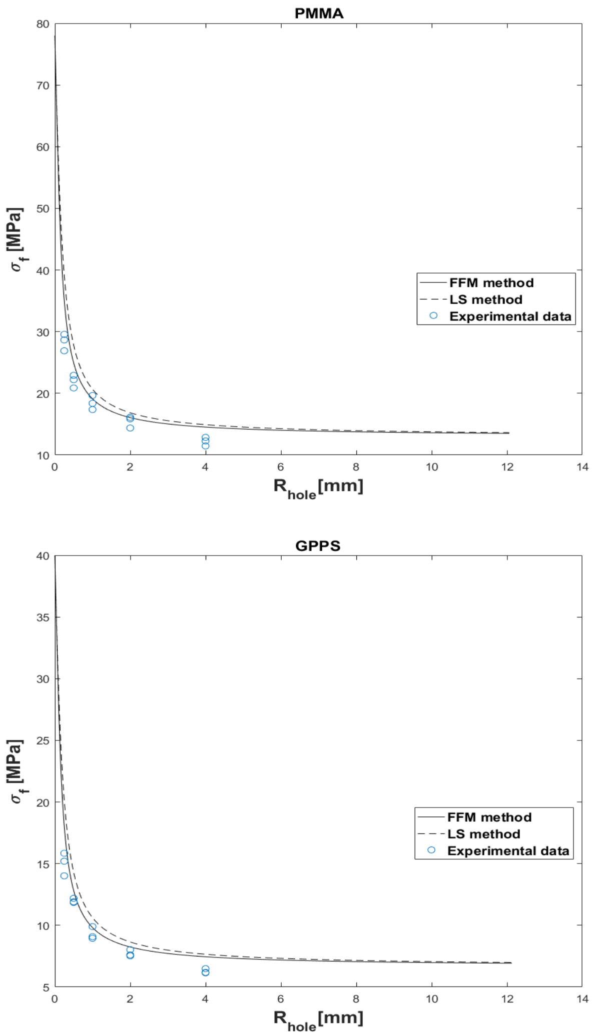

Figure 4.12: Brazilian disk tests, results: experimental data (circle), LS predictions (dashed line), FFM predictions (continuous line)

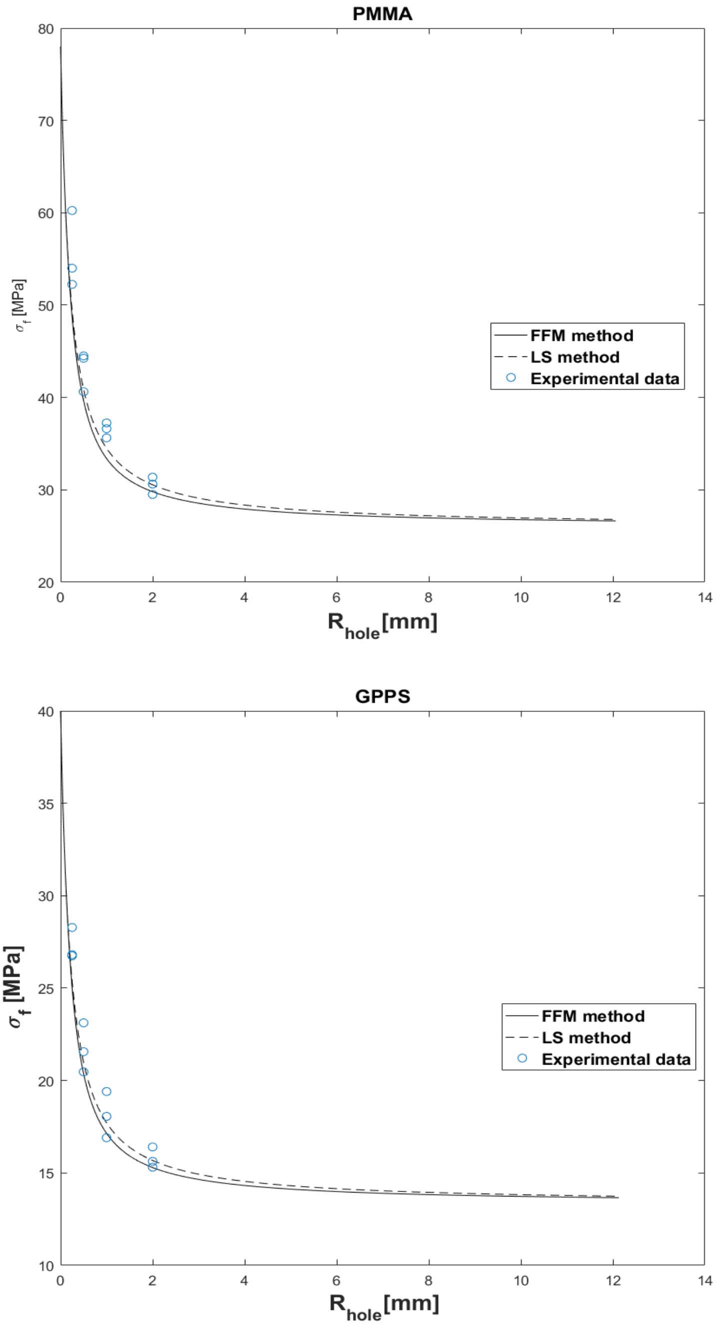

Figure 4.13: Tensile tests, results: experimental data (circle), LS predictions (dashed line), FFM predictions (continuous line)

From the overlying figures it is possible to deduce that, obviously, the stress field decreases as much as the hole radii increase. It is trivial because bigger is the weakness lesser is the load that can bring the collapse of the structural element. Above all the graphs show the great agreement between the experimental values and the numerical ones obtained considering the FFM theory. The two trends almost coincide regardless the material under analysis and the better correspondence is achieved considering the smaller hole radius. This result can be justified taking into account that if the hole dimension is small, the bodies can be assumed as infinite means and so the initial Eq.(3.23), applied to evaluate the stress function used in the LS method, leads to very satisfactory outcomes. As it can be easily perceived good results are also reached considering the tensile plate geometries that show the lesser percentages of error. These percentages are provided in the following graphs:

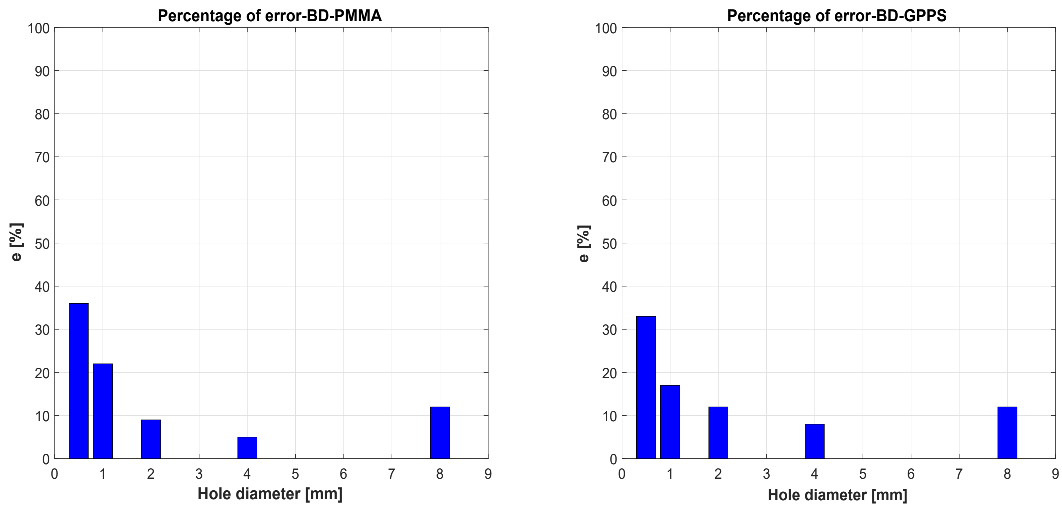

Figure 4.14: PMMA and GPPS BD comparison of results

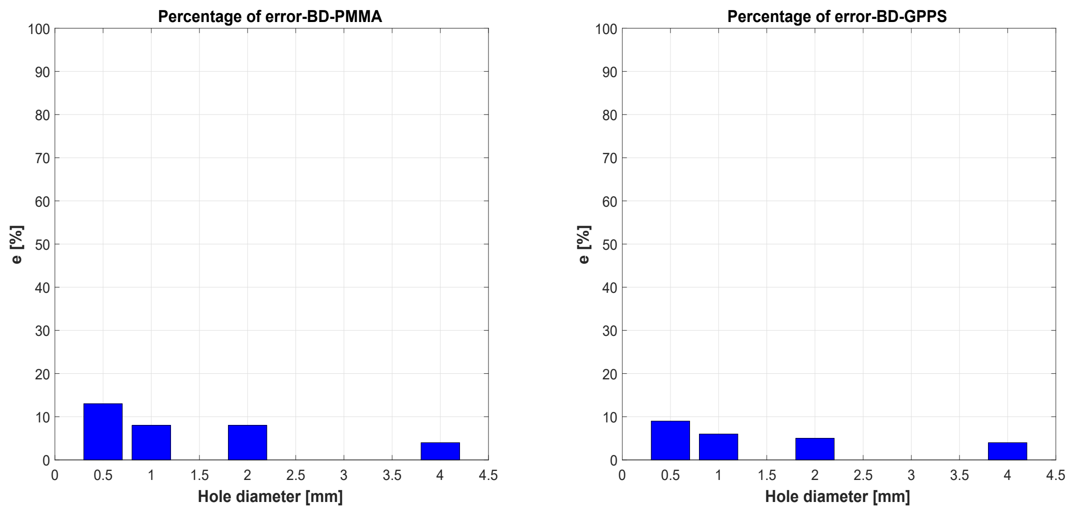

Figure 4.15: PMMA and GPPS tensile plate comparison of results

As it can be seen, the critical load deriving from experimental and numerical analysis are very close, taking into account the bigger hole dimensions. Instead, some differences can be noticed if the smallest diameters are considered and it can be predictable because, in these cases, some plasticization phenomena could take place. The main feature of the graphs that has to be put in evidence is that the percentage of error is under the 12% with the exception of smaller holes for what concerns the brazilian disk geometry. Instead, analyzing the tensile plates, the percentage of error is about the 13% considering the smallest hole dimensions but it is lesser, more or less the 8%, with the other hole diameters. Therefore, it can be asserted that seen analysis fully reflects the great agreement between the experimental and the FFM analysis and that the best correspondence is obtained with the tensile plate geometries.

CHAPTER 5

Conclusions

In this thesis the brittle failure of structural elements characterized by flaws and defects has been analyzed. In particular the effects of the presence of circular holes have been put in evidence. Two different geometries have been studied, the brazilian disk and the tensile plate. For each geometry two different materials (PMMA and GPPS) have been considered and, for all the elements, the hole diameters have been varied from a maximum of 8 mm to a minimum of 0.5 mm. Experimental tests were carried out and the critical load have been obtained. Obviously, bigger is the dimension of the defects lesser is the amount of the load that can be applied until the failure. The holes represent, in fact, a weakness introduced in the structural bodies. Taking into account the smaller hole dimensions it has been seen that the specimens assume a configuration that can be modeled as an infinite geometry. This infinite geometry has been studied with the introduction of the FFM theory. The application of the FFM have made possible to evaluate the stress field and the SIFs, considering different values of the crack extension, of all the specimens. With a finite element analysis, conducted through the ANSYS® code, all the values of interest (σ and K_I) have been extrapolated and they have been compared, respectively, to the experimental and theoretical ones. From the comparison it has been put in evidence that the FFM method is able to obtain results that are every close to the real ones. Indeed, the percentage of error, for what concerns the stress field, is lesser than the 13%, with some exception, for the BD geometry and it is about the 8% for tensile plate geometry (always with the exception of the smallest hole radius). The percentage of

error related to the SIFs evaluation is even lower, reaching a maximum of about the 2% in the BD geometry with the bigger hole radius.
The quality of the outputs are influenced by the dimensions of the flaw and it has to be pointed out that, even if a general brittle behavior is observed, in the surroundings of the holes, especially for what concern the smallest ones, plasticization phenomena can happens. The non-consideration of this feature can slightly alterate the value of the results. These assessments can help to achieve better upshot. Besides it is important to remember another assumption of the above analyses, which is that the material behaves as a homogeneous continuum. In practice, of course, materials are not continuous and for most materials, properties such as strength and toughness are strongly affected by the behaviour at the microstructural level, where features such as grains, precipitates and inclusions exert both positive and negative effects. A fact which is often overlooked is that if stress and strain fields are examinated at this small scale, it can be found that they are strongly inhomogeneous, affected by microstructural parameters such as local grain orientation, disparities in the elastic stiffness of different phases, and the properties of grain boundaries and other interfaces. Experimental measurements (Delaire et al., 2000) and computer models (Bruckner-Foit et al., 2004) have revealed the large extent of these local variations in stress and strain, which can be as high as a factor of 10. These effects may be of relatively little importance if the scale of the fracture process is large – for example, if the size of the plastic zone is much larger than any microstructural feature, in which case it may be satisfactory to think of the stresses calculated by continuum analysis as average quantities, ignoring their local variations. However, the fact is that many failure processes happen on the microstructural scale.

All the criteria used until now, as widely discussed, involve a new structural parameter: the internal length Δ. The evaluation of the latter requires two other parameters to be determined: the flexural strenght σ_u and the fracture toughness (that means the critical stress intensity factor) K_{IC}.

So far a value of $\sigma_u = 78MPa$ for PMMA and a value of $\sigma_u = 40MPa$ for GPPS bodies have been used, properties estimated by some tests carried out by other reaserchers on different specimens, and the value of $K_{IC} = 1.75MPa \cdot m^{0.5}$ again for PMMA and the value of $K_{IC} = 0.9MPa \cdot m^{0.5}$ for GPPS bodies.

The great success of fracture mechanics has been to show that, under certain well-defined conditions, the propagation of the crack can be predicted using some very simple linear elastic analysis. It can possible to predict the conditions necessary for brittle fracture assuming that a crack already exists. If a crack is not present then it will have to be created during the failure. If the crack is already there, on the other hand, we merely have to consider its propagation. A simplifying assumption is that crack growth is under local control, by which we mean that the criteria for propagation can be entirely determined by stress conditions in the immediate vicinity of the crack tip. Within these limitations, the behaviour of the crack can be described using the parameter K_I, the stress intensity factor, which was defined in the previous section where it has be seen that it uniquely determines the magnitude of the stress field in the vicinity of a crack.

The last few decades have seen an enormous rise in computing power and, with it,methods of numerical analysis which allow to simulate complex systems. This has led to a qualitative change in the way in which components are being designed, moving away from simplified analytical calculations and empirical rules towards computer simulations. A computer model has, anyway, important limitation and it can be accurate only if the modeler knowledge is accurate since boundary conditions, as applied loads and restraints, and feature of mesh elements are of primary importance in the representation of the reality and in the deduction of the searched outputs.

In this work it has been analyzed the behavior of brittle elements in the field of the fracture mechanics. Their main characteristic is the focus on a new influencing parameter, the critical distance Δ, that is only a function of the material for what concerns the stress criteria (or equivalently the energetic criteria) and that, instead, is a function of the whole structure when energetic and stress conditions are coupled.
In particular, with the numerical simulation, the line stress method (LS) with the finite element analysis (FEA) was used and taking advantage of the LS+LE criterion the failure of specimens was predicted with a great agreement respect the experimental tests. In fact, to check the validity of these approaches a series of compressive and tensile tests was conducted by a team of reaserchers in Teheran. The tests considered different specimens, circular and rectangular ones, with center hole diameters varying from 8 mm to 0.5 mm for what concerns the disks, and from 4 mm to 0.5 mm for what concerns the rectangular plate. Polymethylmethacrylate and Polystyrene are the material composing the specimens. A total number of 30 specimens for the disks and 24 specimens for the plates were tested. PMMA and GPPS are brittle materials but it is now well known that the brittleness is a property also of the structure and in fact some errors can occur decreasing the geometrical parameters of the samples.
The ANSYS® finite element software was used to achieve the targets in particular to estimate the stresses in the vicinity of the crack-tip and the stress intensity factors. The results were generally satisfactory and the corresponding percentage of errors were very low. The values of the stress intensity factors were also evaluated with the application of the Tada&Paris Handbook (”The stress analysis of cracks”-1973) and an almost perfect agreement was put in evidence.

At the end it is possible to say that while the prediction of failure with the classical theoretical analysis can be obtained only for few particular geometries and under precise characteristics (stress criterion-no crack present and energy criterion-large crack present) the application of the finite fracture mechanics covers a wider field of situations. With the exploitation of the new finite element softwares the desired outputs can be obtained more easily.

Bibliography

ANSYS® Academic Research Mechanical, Release 16.2, Help System, Analysis Guide, ANSYS, Inc.

ASM International, *Tensile testing*, Second Edition, 2004

ASTM D3967-08, *Standard Test Method for Splitting Tensile Strength of Intact Rock Core Specimens*, 2008

Carpinteri A., *Scienza delle Costruzioni*, Pitagora Editrice Bologna, 1992

Carpinteri A., *Meccanica dei materiali e della frattura*, Pitagora Editrice Bologna, 1992

Carpinteri A., Cornetti P., Pugno N., Sapora A., Taylor D., *A finite fracture mechanics approach to structures with sharp V-notches*, Engng Fract Mech, 75 (2008) 1736-1752

Carpinteri A., Cornetti P., Pugno N., Taylor D., *Finite fracture mechanics: a coupled stress and energy criterion*, Engng Fract Mech, 73 (2006) 2021-2033

Leguillon D., *Strength or toughness? A criterion for onset at a notch.*, Eur J Of Mech A/Solids, 2002 61-72

Tada H., Paris PC, Irwin GR, *The stress analysis of cracks handbook*, Third Edition. Paris Production Incorporated, 2000

Taylor D., *The theory of critical distances - A new perspective in fracture mechanics*, Elsevier Oxford, 2007